

Chapter 1

Introduction

With the progress of technology, the demand for the energy is more and more. The consumption of the energy is expected to increase outstandingly at the future day. That will make the global energy system and ecological environment bear the enormous pressure. In order to improve energy service efficiency and reduce the energy wastes, improving the lighting equipment is the most important. LED is the key point. LEDs offer benefits such as small size, long lamp life, low heat output, energy savings and durability. Hence all the light bulbs and fluorescent lamps will be replaced by LED due to the high efficiency of luminescence. White light LEDs, however, currently do not produce enough lumen output to make them competitive with many general light sources. White light LED feature a phosphor added to a blue LED that converts some of the light emission into yellow, resulting in a bluish-white light. This restricts their use in architectural projects to applications where small lumen packages are needed. So promoting the efficiency of lighting of semiconductor materials is the most important thing for improving small lumen packages. Hence the efficiency of lighting of GaN, the semiconductor of blue LED chip, is the key problem.

GaN has attracted increasing interest for device use in electronic device, light-emitting diodes (LEDs) and laser diode owing to the great band-gap for a long time.^{[2][3][4]} The band-gap of GaN is 3.4 eV at room temperature.^[1] With the arrival of nanotechnology times, we have great

interest in the change of GaN characteristic while the scale become more and more small. In research of GaN nanostructure, a number of groups synthesize GaN nanowires successfully using different ways such as carbon nanotube confined reaction^[5](Fig.1-1), arc discharge^[6](Fig.1-2) laser ablation^[7](Fig.1-3), sublimation^[8](Fig.1-4), pyrolysis^[9](Fig.1-5), and chemical vapor deposition^{[10]~[15]}(Fig.1-6~1-9). They have the similar problem, that is the diameter of GaN un-control and larger.

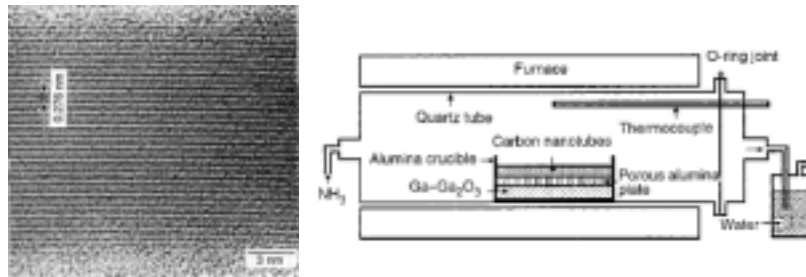


Fig. 1-1 Gallium nitride nanorods were prepared through a carbon nanotube-confined reaction. XRD pattern, diffraction patterns and HR image of wurtzite GaN nanorod

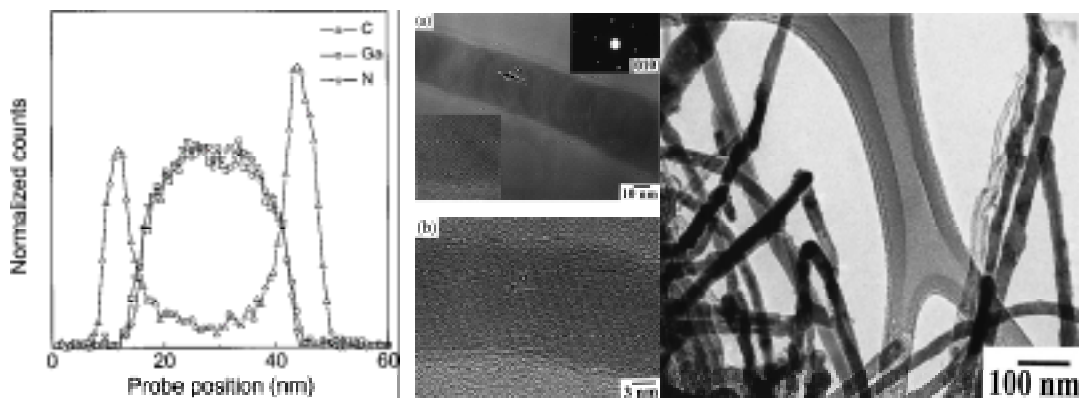


Fig.1-2 A method using an arc discharge in a nitrogen atmosphere for synthesizing large quantities of GaN–Carbon composite nanotubes and GaN nanorods.

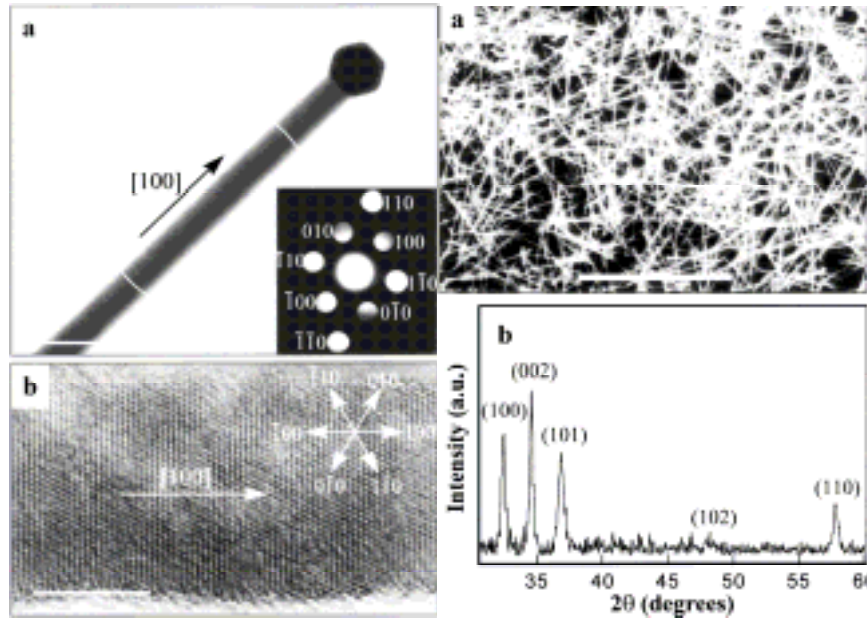


Fig.1-3 Laser-Assisted catalytic growth of single crystal GaN nanowires

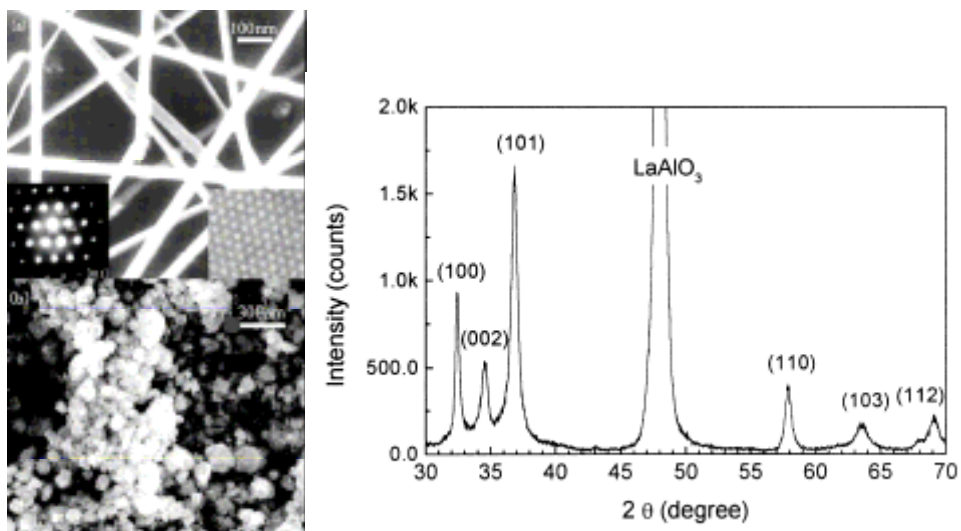


Fig.1-4 Formation of GaN nanorods by a sublimation method.

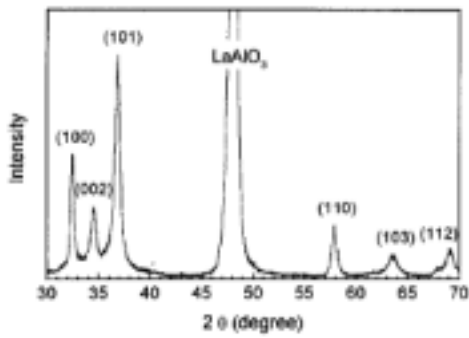
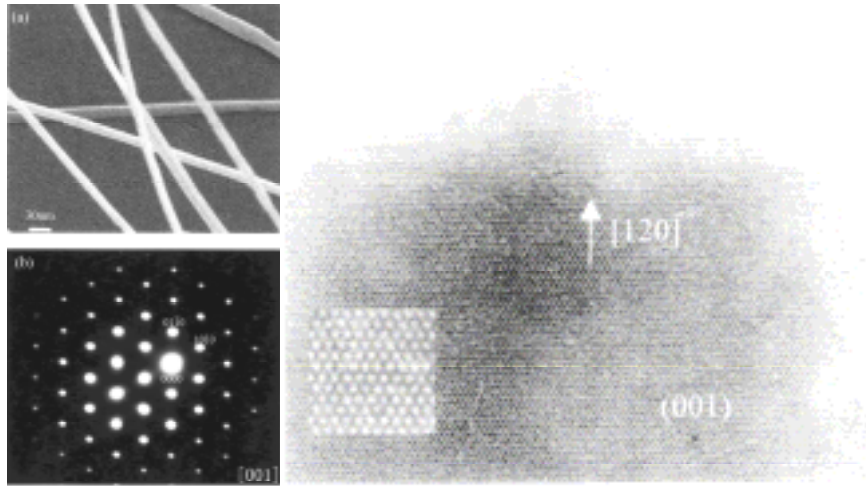


Fig.1-5 Straight and Smooth GaN Nanowires

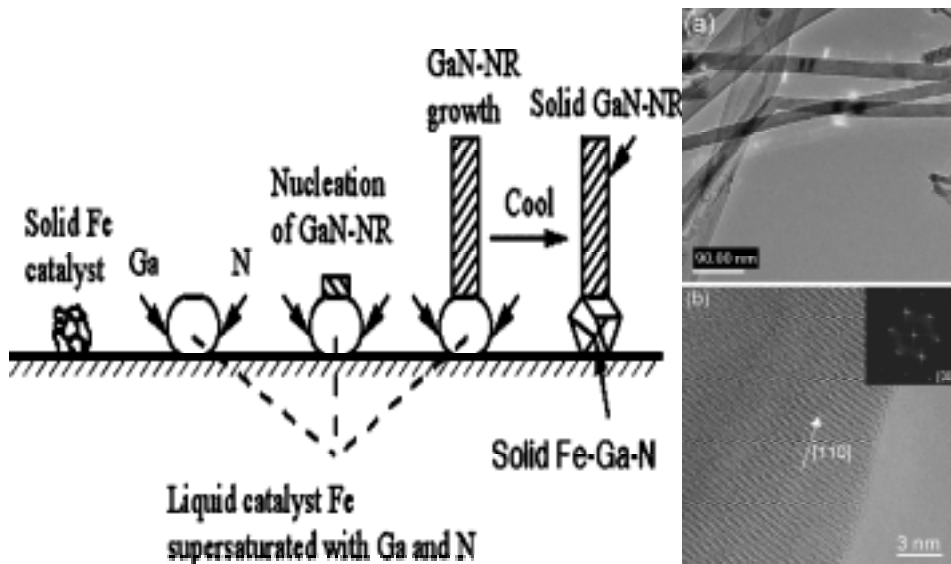


Fig.1-6 Pyrolysis approach to the synthesis of gallium nitride nanorods

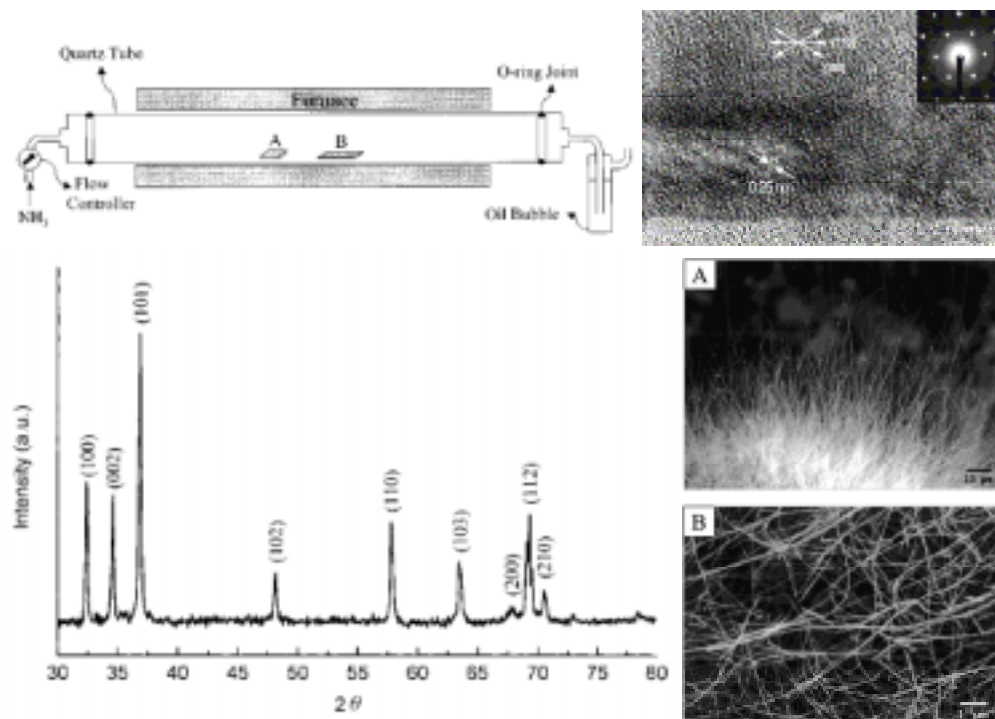


Fig.1-7 Catalytic growth and characterization of gallium nitride nanowires

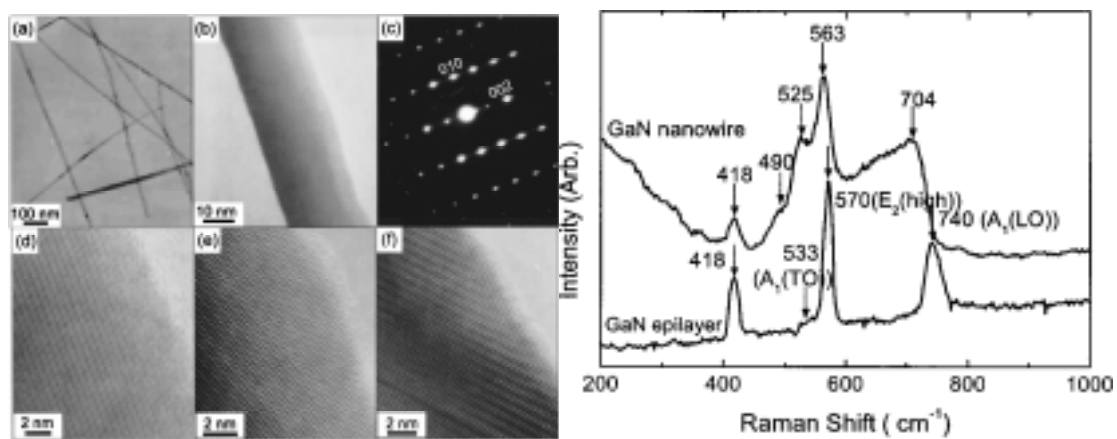


Fig.1-8 Strained gallium nitride nanowires

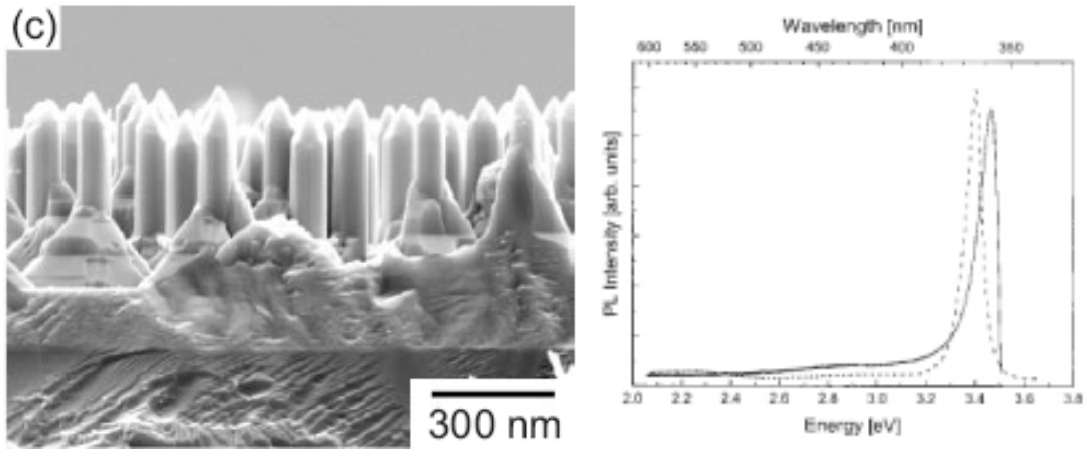


Fig.1-9 Growth of GaN nanorods by a hydride vapor phase epitaxy method

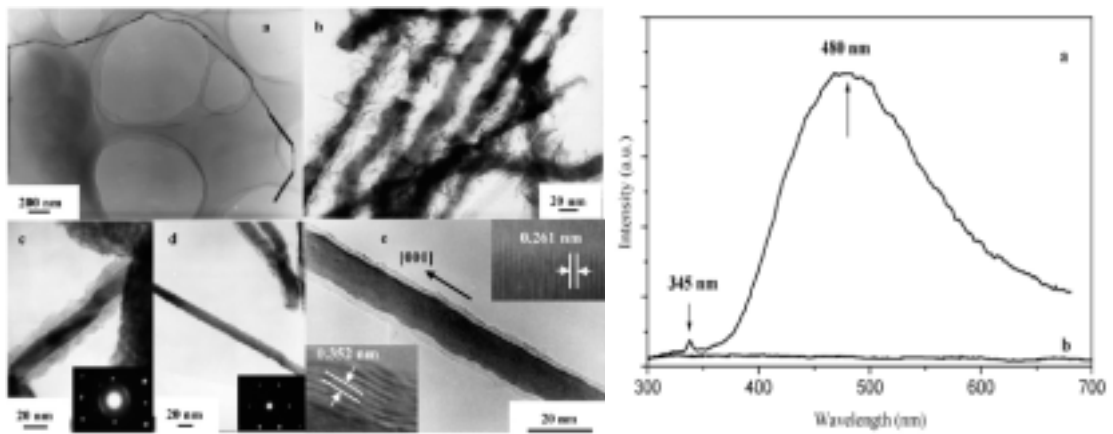


Fig.1-10 A HRTEM image and Photoluminescence spectra of the 1-D GaN-SiO₂ nanocable

Quantum confinement effects can be observed at the semiconductor materials while the diameter is small enough. And that it will affect the

characteristics of materials, such as optic and electronic properties. For example, GaN will have higher light-emitting efficiency while the dimension reduces such as quantum well. The LEDs chip is one of important applications of quantum confinement effect. Although LEDs chip have been produced well and economical at present, we want to develop a novel method for synthesizing a higher light-emitting efficiency GaN. So we use CNT to assist in synthesizing 1-D or 0-D GaN. In this thesis, we use CNT as a template that will provide a new approach to synthesize quantum dot or wire of GaN.

1-1 The develop of blue light-emitting materials and Gallium Nitride

Since the invention of the incandescent electric lamp by Thomas Edison in 1879, there has been a brighter lighting source. With the technological growth, the light source has most recent advancement. The recent revolution is the lighting advancement light-emitting diode (LED).^[16] (Fig.1-11(a)(b)) The color LED with light emission efficiencies superior to incandescent lamps ,and their commercially importance has increased by the early 1990s^[17] as shown in Fig. 1-13, Table 1-1. However, LED emit light at shorter wavelengths within the visible spectrum is a big challenge. Although successfully synthesizing LEDs and LDs with SiC and - materials have been synthesized, the device has been abandoned due to the very low efficiency in SiC^[18] and the short lifetime in - materials. As a result, the III-V nitride materials possessed of a direct transition band gap energy ranging from 1.9 eV for InN, to 3.4eV

for GaN, to 6.2 eV for AlN at room temperature^{[19][20]}(Fig. 1-12) as well as the single-crystalline GaN nanowires and nanotubes^[21] (Fig.1-14) has been showed for realizing photonic and biological nanodevices such as blue-light-emitting diodes, short wavelength ultraviolet nanolaser,^{[22][23]}

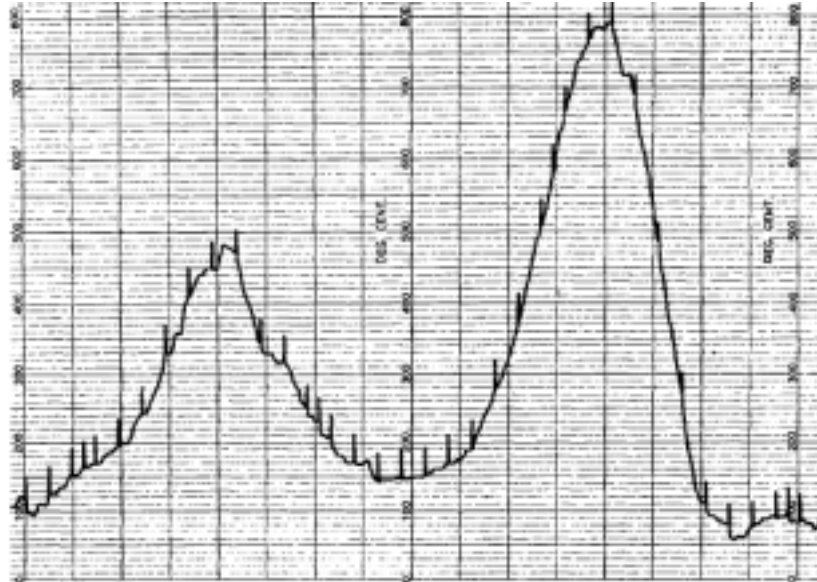


Fig.1-11(a) Radiation from a forward biased p-n junction at 78°k. The band at the left is at 1eV and is caused by some impurity. The band at the right is edge emission which peaks at 1.47eV at 78°k.

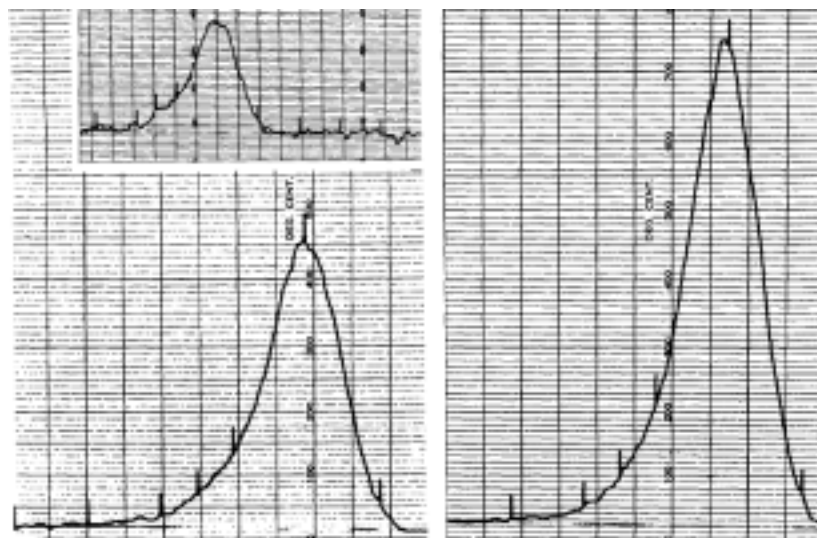


Fig.1-11(b) The band edge radiation at 1.47eV as a function of current at 0.2 (upper left), 0.5 (lower left), and 0.8 A(right), in a diode of area $2 \times 10^{-2} \text{ cm}^2$. The intensity of radiation is proportional to the current. The width at half-maximum is 0.017 eV .

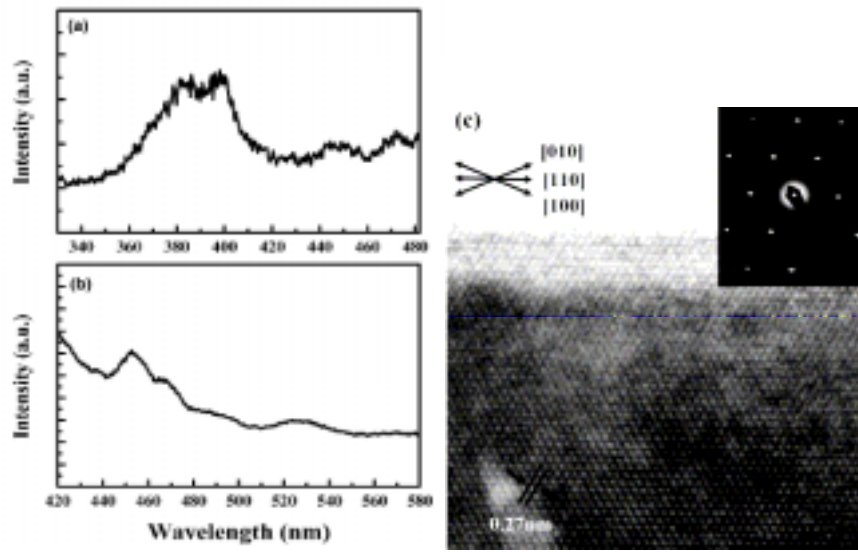


Fig.1-12 PL spectra of the GaN nanowires with an excitation wavelength of (a) 254 and (b) 325 nm. (c) HRTEM image of the straight portion of the nanowire and the corresponding electron diffraction pattern (inset)

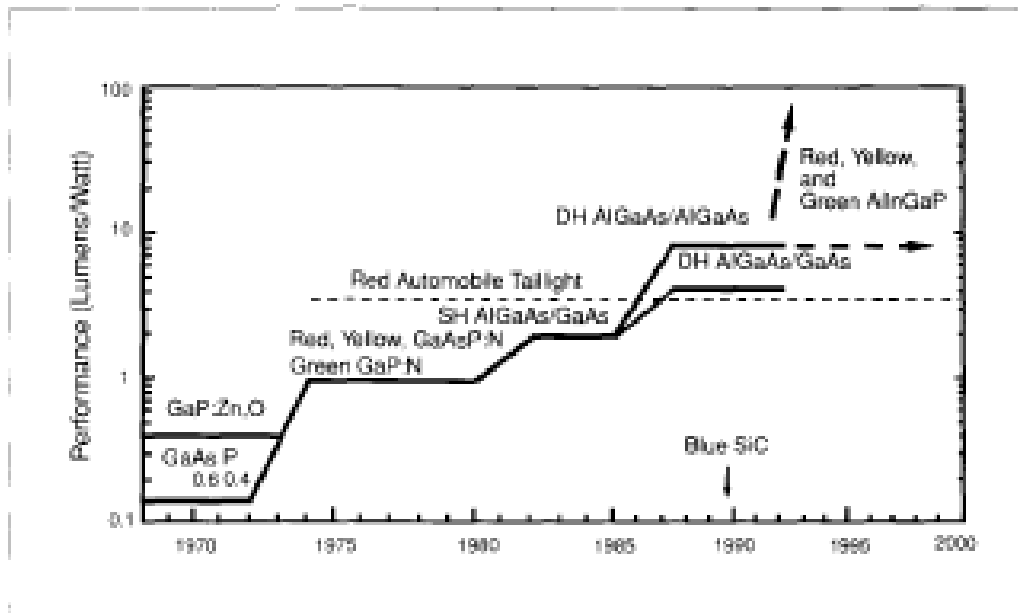


Fig. 1-13 The development of various type LEDs

Table: Characteristics of Visible LEDs							
LED TYPE	COLOR (Peak Wavelength)	PRODUCTION METHOD	STRUCTURE*	BANDGAP TYPE	LATTICE MATCHED	TYPICAL EXTERNAL QUANTUM EFF. %	TYPICAL PERFORMANCE (lumens/watt)
GaAsP	Red(650)	VPE + Diffusion	HJ	Direct	No	0.2	0.15
GaP:ZnO	Red (700)	LPE	HJ	Indirect	Yes	2	0.4
GaAsP-N	Red (630)	VPE + Diffusion	HJ	Indirect	No	0.7	1
GaAsP-N	Yellow (585)	VPE + Diffusion	HJ	Indirect	No	0.2	1
GaP-N	Yellow-Green (565)	LPE	HJ	Indirect	Yes	0.4	2.5
GaP	Pure Green (555)	LPE	HJ	Indirect	Yes	0.1	0.6
AlGaAs	Red (650)	LPE	SH	Direct	Yes	4	2
	Red (650)	LPE	DH	Direct	Yes	8	4
	Red (650)	LPE	DH-TS	Direct	Yes	16	8
AlInGaP	Orange (620)	MOCVD	DH	Direct	Yes	6**	20**
	Yellow (585)	MOCVD	DH	Direct	Yes	5**	20**
	Green (570)	MOCVD	DH	Direct	Yes	1**	6**
SiC	Blue (460)	MOCVD	HJ	Indirect	Yes	0.02	0.04

* HJ Homojunction
SH Single Heterostructure
DH Double Heterostructure
DH-TS Double Heterostructure, transparent epitaxially-grown substrate.
** Best reported results [5]. Typical commercial performance not established.

Table 1-1 Different types of LEDs are grown with different techniques and have different characteristics.

(Fig 1-15) and nanofluidic biochemical sensors. Gallium nitride with a robust wide band-gap, high melting point, high carrier mobility, and high electrical breakdown field, and it is a good semiconductor material for using in high-performance, high-power optoelectronic devices.^[24](Fig. 1-16) Moreover, Nichia Chemical Industries (Anan, Tokushima-ken, Japan), announced commercial blue GaN LEDs in November 1993 and green LEDs in September 1995. The discoverer, Shuji Nakamura^[25], has pushed the LEDs continue to into the full-color outdoor display, traffic signal, exterior lighting and automotive interior markets. As shown in Table 1-2, the development of blue light-emitting materials and GaN.

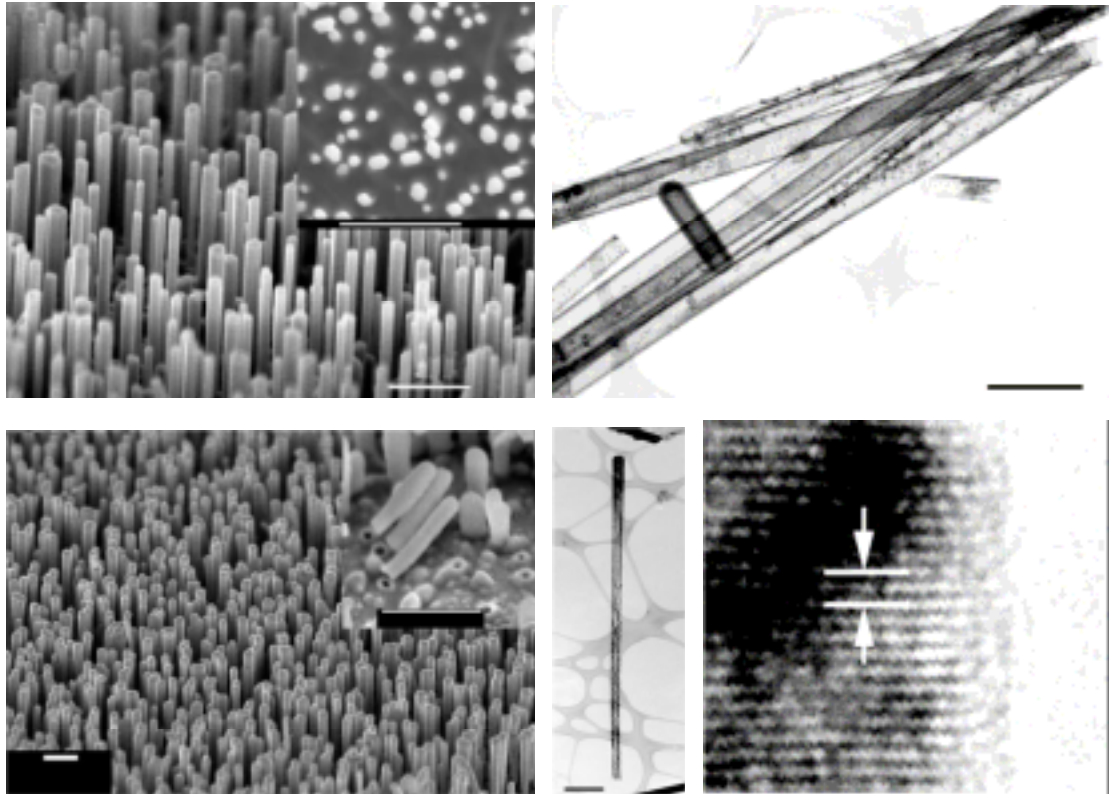


Fig.1-14 Arrays of ZnO nanowires and GaN nanotubes. Shown are SEM images of the ZnO nanowire template arrays. Structural characterization of GaN nanotubes, TEM images of the GaN nanotubes.

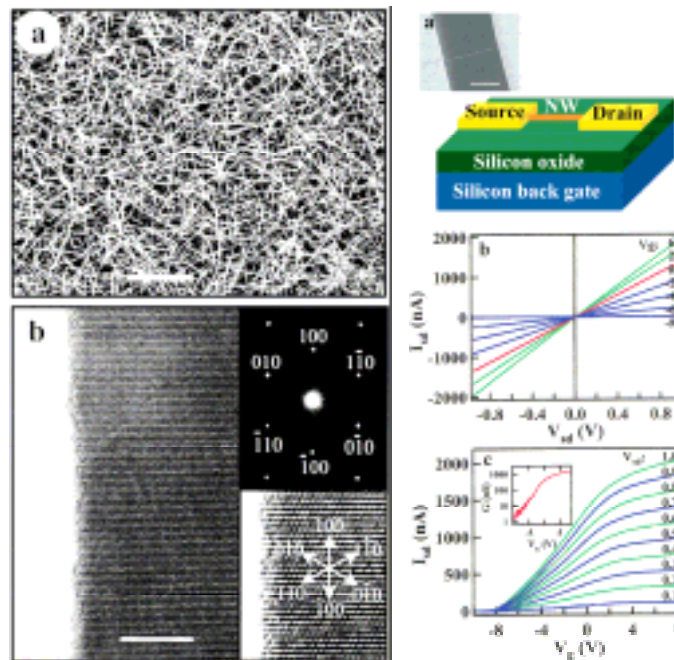


Fig.1-15 FE-SEM and TEM image of GaN NWs. The electron diffraction pattern was recorded along the (001) zone axis. (Upper right corner) Schematic of a NW FET, and (inset) FE-SEM image of a GaN NW FET.

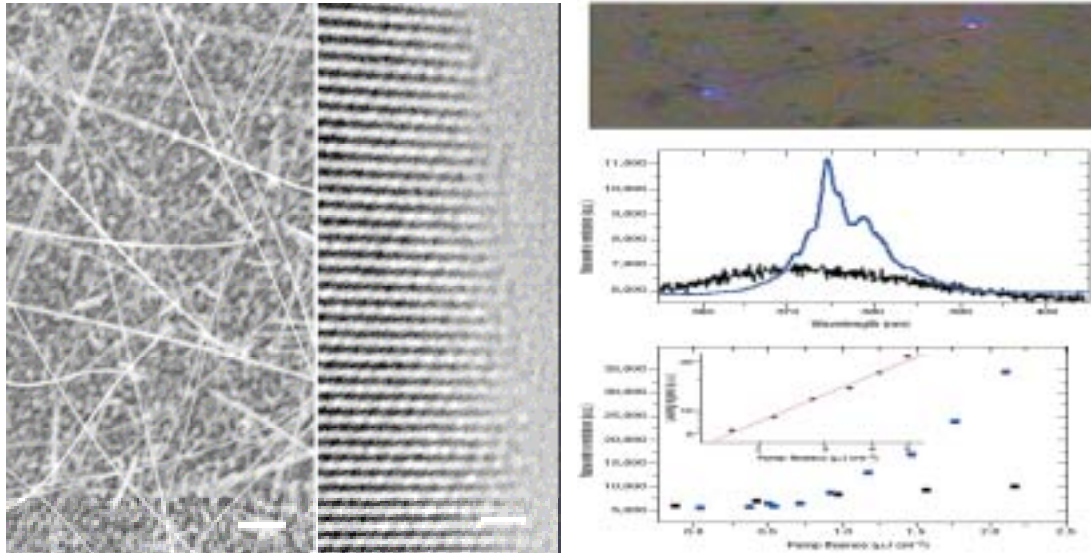


Fig.1-16 Electron microscopy images of synthesized GaN nanowires and individual,isolated GaN nanowire laser.

Table 1-2 The develop of III-nitride materials.

TIME	Develop of III-V nitride materials ^[42]
1907	The first III-nitride material, AlN, has been synthesized.
1937	Solving GaN crystalline structure.
1969	Synthesizing GaN thin film.
1971	<ol style="list-style-type: none"> 1. The first metal-insulator-semiconductor LEDs being synthesized with GaN thin film by Pankove. 2. Manasevit successfully synthesize GaN thin film by metal organic chemical vapor deposition. 3. Acicular GaN is synthesized by Dingle and getting the ultraviolet radiative spectrum of GaN at 2K. 4. R. Dingle etc.^[26](Bell Laboratory, American) find the single

	crystal needle-like GaN has excite radiation and laser behavior at photon energy 3.45 eV.
1972~ 1982	Develop stop 1. Lack the suitable substrate 2. It is synthesized hardly in p-type GaN semiconductor and can not control the conductivity of n-type GaN. 3. Synthesizing AlGaN and InGaN thin film that is difficultly.
1983	Yoshida, he synthesize GaN thin film on suitable AlN buffer layer to overcome the difference of lattice constant between substrate and GaN on purpose. Moreover the structure enhances the luminescence efficiency of GaN thin film.
1986	Akasaki and Amamo, they grow up AlN buffer layer on sapphire (α -Al ₂ O ₃) with low temperature and advance the luminescence efficiency and conductivity of thin film at the same time. Akasaki show the truth by using SiH ₄ affect the n-type doping. He found p-type GaN doped Mg has no ability to carry electric hole. That maybe is the hydrogen of SiH ₄ separate GaN and doping material, cause hole unable to move. GaAs and InP have the same situation.
1989	Amano and Akasaki, they active GaN thin film doped Mg by low-energy electron-beam irradiation. It result in high impedance membrane turn into the electric hole with high thickness and the first one p-n junction blue light-emitting diodes synthesized successfully.
1991	1. Nakamura grew thin, low-temperature AlN layer and, later,

	<p>amorphous GaN buffer layers facilitated the growth of high-quality GaN films on sapphire substrates by metal-organic chemical vapor deposition (MOCVD). That would reduce the mismatch of lattice constants between GaN thin film and substrate. Nakamura improving the hot convection question at high growth temperatures with two-flow reactor equipment as well as that push the reactant to the substrate surface with the assisting gas from normal direction of substrate. The assisting gas will improve the quality of thin film.</p> <p>2. M. Asif Khan etc. ^[27] discover that GaN was excited radiation on the normal direction of epitaxy phase at room temperature.</p>
1992	Nakamura annealed GaN under N ₂ flow for improving the reduction in efficiency of light emitting.
1993	Nichia plans to produce blue light-emitting diodes.
1994	Nakamura developed the light-emitting diodes which completed the range of visible light LED.
1996	Nakamura developed the blue light-emitting semiconductor laser which has continuous light wave. ^[28]
1998	Japanese industry, Korea S., Taiwan follows up. Technological transformation industry of National Chiao Tung University of Taiwan.

1-2 Nanomaterial and quantum confinement effect

We can find the importance of the material diameter from the talk of Richard Feynman, winner of Nobel Prize for physics, refer to during a speech, “If the mankind can come up to process materials and make the component in atomic dimension, we will have a lot of inspiring new discoveries.” Besides owing to the quantum energy level of thin metal particle will change with the diameter was discovered by Kubo at 1962 (professional of thermodynamics, Japan). The special characteristic of thin metal particle begins to be paid a great attention.

The definition of nanomaterial is that the size between 1 and 100 nanometer. Its characters are:

1. There is molecule scale structure which is different from the crystal or amorphous structure.
2. The characteristic of nanomaterial are different from traditional crystalline grain or the non-brilliant quality material, for instance the nature, such as optics^[29], magnetic , heat spreading ^{[30][31]}, spreading^{[32][33][34]} and machinery^[35], etc.

The quantum energy level of nanomaterial is different from the block by the limitation of degrees (Fig. 1-17). The quantum energy level of nanomaterial is not continuous near the Fermi Level owing to the density of molecule is less than bulk, so the gap of energy level become larger than bulk while the dimension decrease at the same time as shown in the following equation :

$$E=n^2h^2/8 mL^2$$

$$E=h \nu =hc/\lambda$$

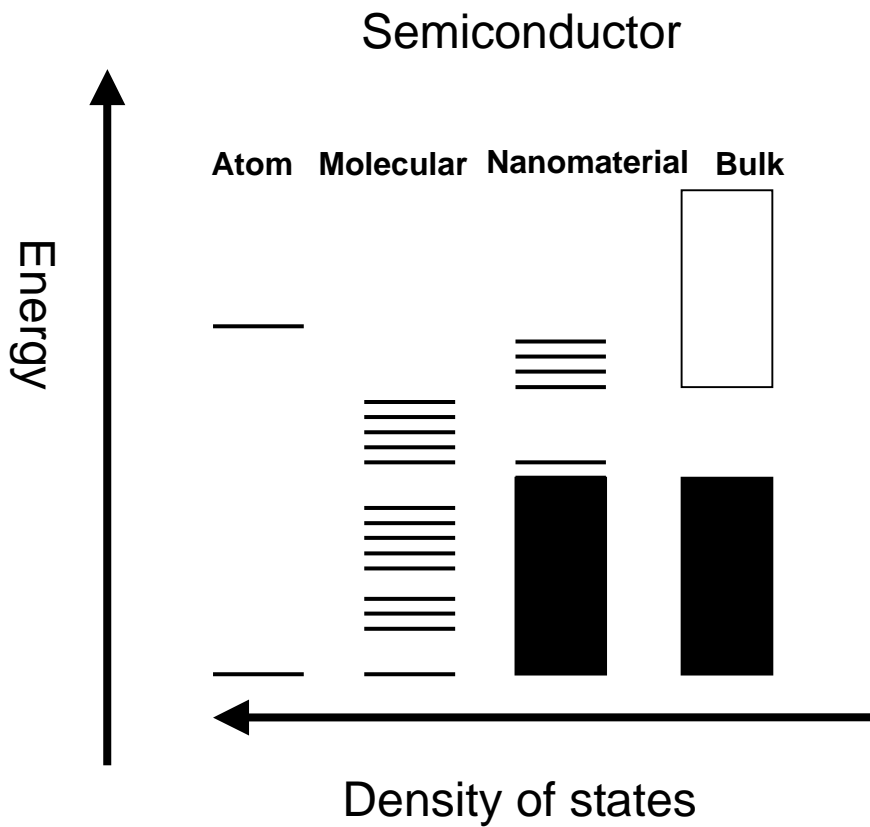


Fig.1-17 Change of energy-level of atom, molecular, nanomaterial and bulk

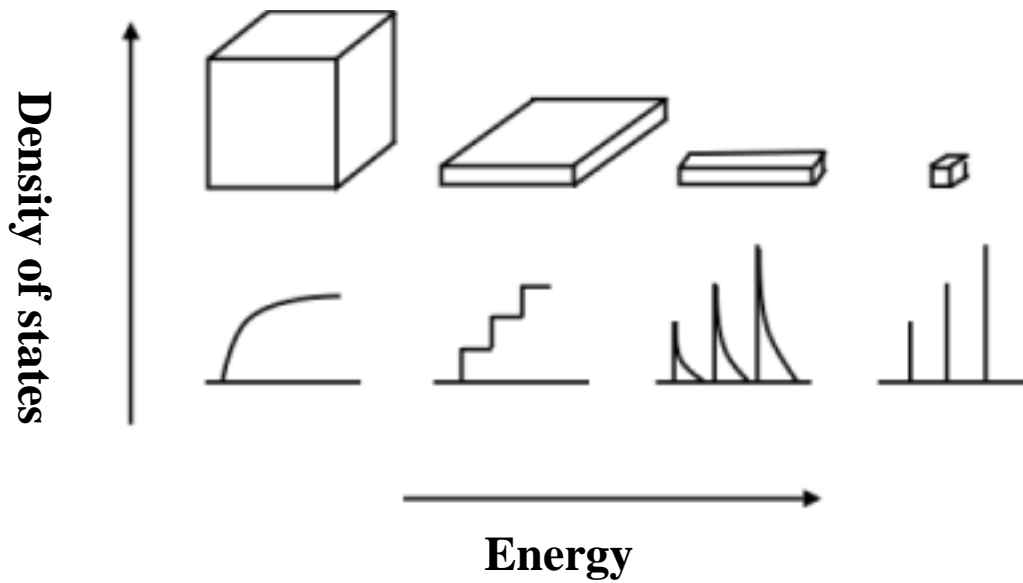


Fig.1-18 The relationship between the form and density of state

Where the L is the diameter of nanomaterial, λ is wavelength of photon, n is the different quantum energy level. While the diameter is more and more small and the gap of energy level become larger, the wavelength of adsorption spectrum will has short shift.

Semiconductor nanomaterials can be divided into (1) quantum dot; (2) one dimension nanomaterials; (3) two dimension quantum well; (4) bulk (Fig. 1-18) by dimension and density of state. Several characteristics of nanomaterial are different with bulk, for example, intensity of material, modulus, ductility, wear and tear, magnetism characteristic, surface catalysis and corroding etc. In fact, there has been already existing nanomaterial in the nature, for example, lotus and navigation feature of the honeybee

The effect of surface and interface become more important while the reducing of material dimension and the number of surface atom getting more and more. The quantum confinement effect will more noticeable while the diameter is smaller than Bohr's radius It will be remarkable such as optical, quantum energy level and the other properties. For instance, absorbed spectrum has red or purple shift and what is caused by the quantum confinement effect.

Quantum confinement effect cause more change in physics characteristics. The melting point of gold is 1064°C at normal state, for example, which will reduce by 27°C while the diameter of gold even as small as 10 nm and the melting point only has 327°C in 2 nm; the band-gap of CdSe change from 1.7eV to 2.4eV with the diameter change from 20nm to 2nm; the threshold temperature of superconductivity rise; silver is provided with spin or spin glass etc.. So the gap of quantum

energy level will be controlled by controlling the diameter of materials as well as we can control the threshold temperature or more physics properties even.

1-3 Carbon nanotube

Carbon nanotube is famous one of new materials synthesized by nanotechnology. Carbon can be divided into five kinds :(1) Diamond; (2) Graphite; (3) Charcoal; (4) Fullerene; (5) Carbon nanotube (Fig. 1-19(a)~(e)). Carbon nanotube was discovered in 1991 by the Japanese electron microscopist Sumio Iijima(NEC company) in multi-wall form (Fig.1-20) while he was studying the material deposited on the cathode during the arc-evaporation synthesis of Buckyball.

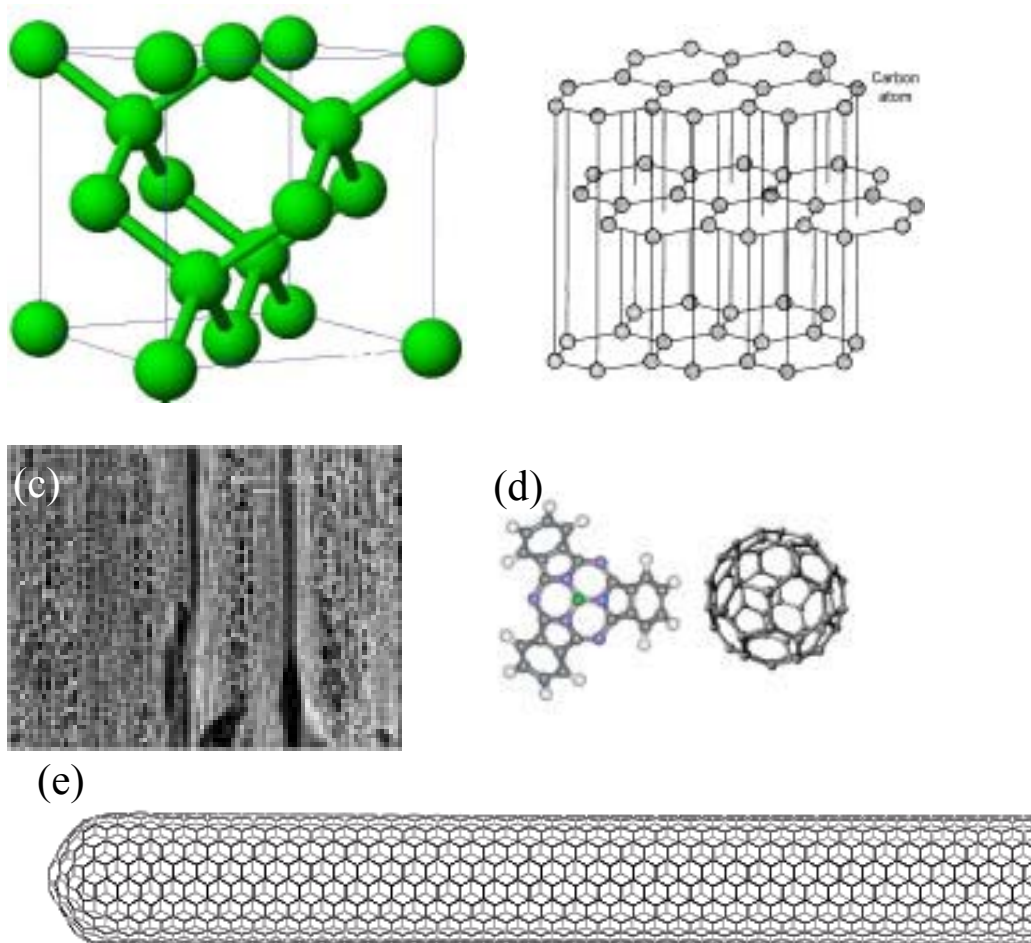


Fig.1-19 The different shape of carbon (a) diamond (b) graphite (c) charcoal (d) fullerene (e) carbon nanotube

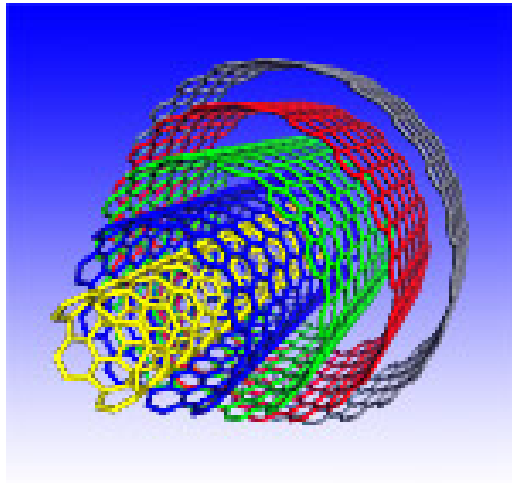


Fig.1-20 Multi-wall carbon nanotube

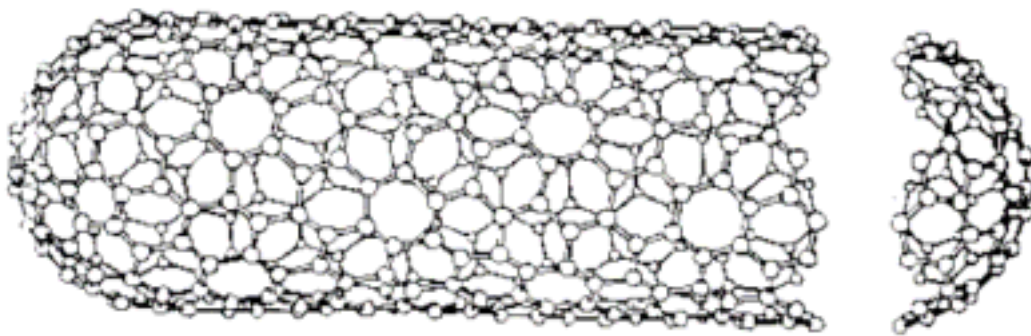
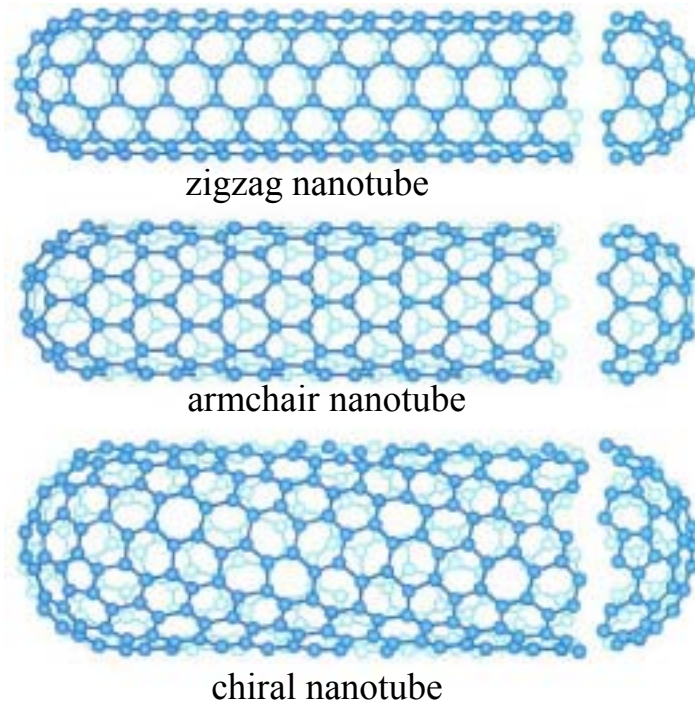


Fig.1-21 Single-wall carbon nanotube



Single-wall nanotube was synthesized in 1993 presently as shown in Fig. 1-21 the structure of single-wall carbon nanotube is empty and consists of steady ring carbon. A single-walled carbon nanotube can be looked as a single layer sheet of graphite or as single molecule. So the characteristic of graphite will influence carbon nanotube by the direction of graphite rolled into a cylinder, a special direction is selected, the direction along the axis of the nanotube^[36].(Fig.1-22)

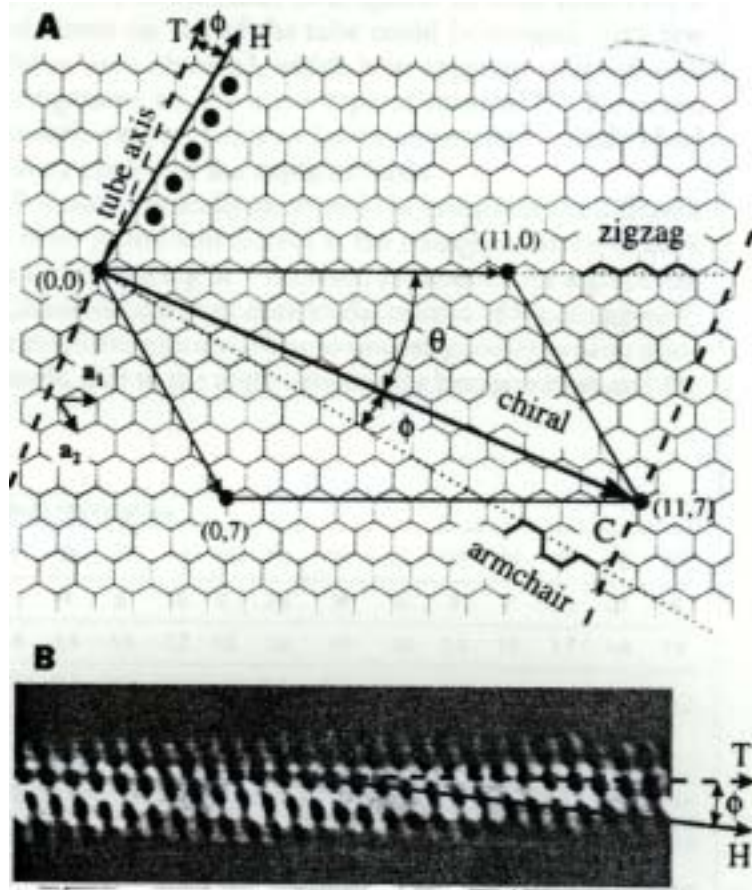


Fig.1-22 The direction of graphite rolled into a cylinder

The structure of carbon nanotubes was determined by the Wrapping Vector (Fig. 1-22):

$$C = na_1 + ma_2;$$

where n and m are integers of the vector, a_1 and a_2 are unit vector

The characteristics of carbon nanotube were determined by the angle of wrapping and the diameter:

$$D = (\sqrt{3}/\pi) a_{c-c} (m^2 + nm + n^2)^{1/2}$$

$$\theta = \tan^{-1} [\sqrt{3} / (2m + n)]$$

where a_{c-c} is the distance between carbon and carbon atom in graphite

If $n=m$, $\theta=30^\circ$ the nanotube is an armchair structure.

If $m=0$ or $n=0$, the nanotube structure is zigzag, $n-m=3N$. (N is integral)

If $m=0$ or $n=0$, and the wrapping angle is between 0° and 30° , the nanotube has chiral symmetry.

The values of n and m determine the chirality, or wrapping of the nanotube. The chirality in turn affects the conductance of the nanotube, density, lattice structure, and other properties. The single-wall carbon nanotube is considered to be metallic if the division of the value $n-m$ is $3N$ (where N is integer). On the other hand, the carbon nanotube is semi-conducting while that is not $3N$.^[37]

Carbon nanotube have many special and excellent properties, for example, the tensile strength is 100 times higher than that of steel; young's modulus~1TPa (same as diamond); high thermal conductivity (in principle); ductile (fracture strain~5-10%) ; unique structure / geometry; diameter: 1-50nm length: 1-10micron; structural perfection (in principle) emission threshold~1 V/um^[43]. Table 1-3^{[43][38]} shows the comparison of carbon nanotube, steel and wood. These researches make an explosion about physical and chemical properties of carbon nanotubes in materials

Materials	Young's Modulus (GPa)	Tensile strength (GPa)	Density (g/cm ³)
Single-walled CNT	1054	~150	
Multi-walled CNT	1200	~150	2.6
Steel	208	0.4	7.8
Wood	16	0.08	0.6

Table 1-3 The comparison of carbon nanotube, steel and wood

1-4 Motivation

GaN nanowires and nanodots have been synthesized successfully by many different ways and their characteristics have already been studied for a long time. Although these methods and characteristics already knew very well, their diameter and quality of GaN can not be controlled.

We try to synthesize GaN nanowire by the confinement of carbon nanotube that is different from Han et al. We hope that carbon nanotube can working as pattern. Carbon nanotube is used for limitation of the

epitaxially laterally overgrowth (ELOG) of GaN. Quantum wire of GaN is synthesized by using carbon nanotube.

Beside confined the diameter of GaN by using carbon nanotube, we synthesize successfully the needly GaN. That is small enough to observe quantum confinement effect. Furthermore we try to control it's length, let the effect be more obvious.

Chapter 2: Experimental Method

2-1 Introduction

MOCVD system has been used for a long time. In this study, metal-organic source (TMG) was injected into the low-pressure chemical vapor deposition system.

2-2 MOCVD system

Chemical Vapor Deposition method is an important technique on nanowire synthesis, which offers an economical and efficient ways in composing semiconductor materials. In this investigation, the GaN and GaN@CNT nanostructure was synthesized by using low-pressure metal-organic chemical vapor deposition (MOCVD) (Fig.2-1) system.

The reaction is thermally driven and the use of sub-atmospheric pressure permits a relatively low deposition temperature in metal-organic chemical vapor deposition technique. Moreover, a uniform temperature at low pressure leads to excellent uniformity of film thickness and composition. In this study, the different wire was synthesized by changing experimental condition, including growth temperature, gas flow, component of the reacting gas, temperature of metal-organic source and growth pressure, etc. The details of system equipments are shown in Fig. 2-1.

2-2-1 Gas and Metal-Organic sources

The gas of MOCVD system is injected respectively into main chamber by pipe. C_2H_2 , NH_3 , and trimethylgallium (TMG) gases were used as C, N and Ga precursors respectively. The flow rates of all gases were controlled by mass flow controller (MFC).

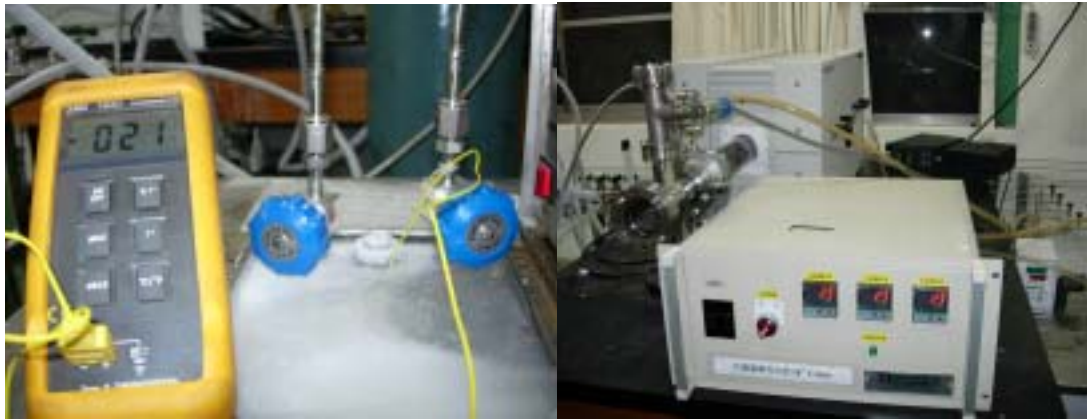
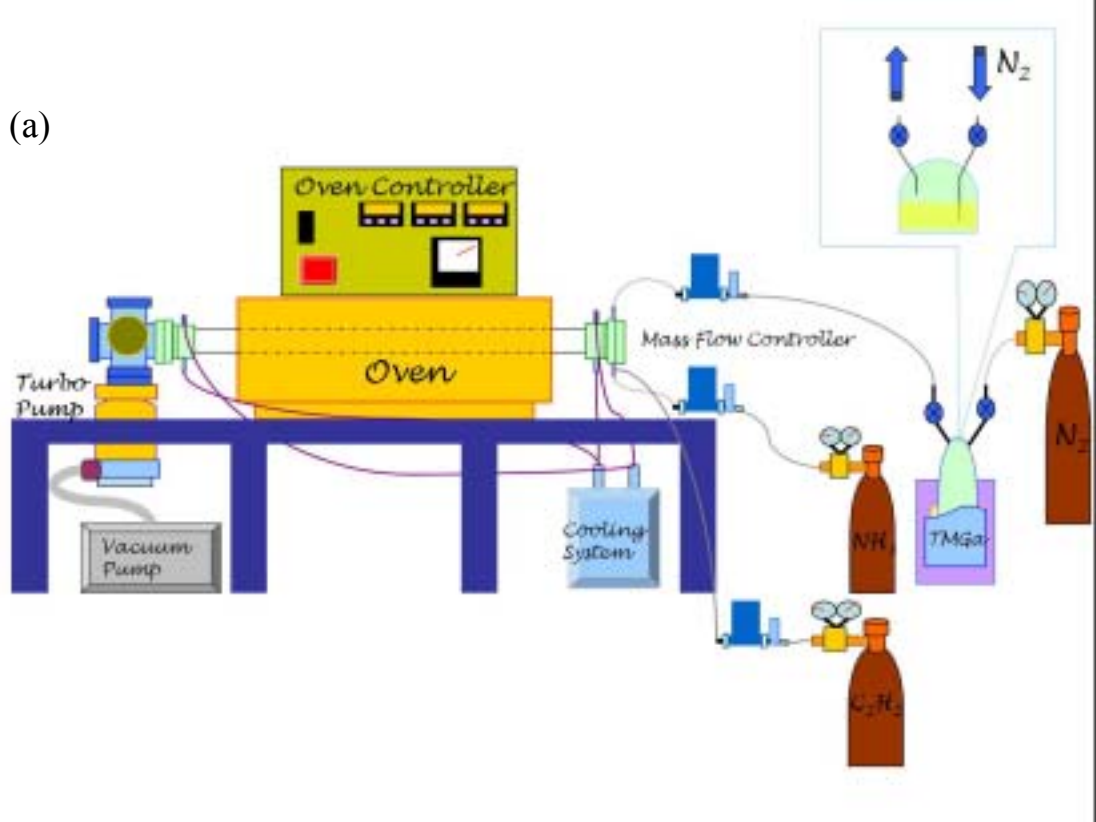


Fig.2-1(a) Schematic diagram of MOCVD system (b) Pictures of TMGa source and high temperature oven

2-2-2 Deposition chamber

A quartz tube with 2.5 inches diameter is used as a reaction chamber. It contains a gas inject port, a sample substrate holder, a heater source (maximum temperature 1200 °C), and a pumping connection port.

2-2-3 Pumping system

The MOCVD system has two pumps. They contain a turbo-molecular pump (pumping speed 1100 liter/sec) and a mechanical pump. The mechanical pump can evacuate the chamber to about 10^{-3} Torr and this pump system can evacuate the chamber to a base pressure of 1×10^{-6} Torr. All pressure is measured by a cold cathode gauge.

2-3 Experiment procedures

2-3-1 Substrate preparation

- (1) Cleaning the silicon (100) substrate by spurting N_2 gas.
- (2) 5nm-thick Au thin film was sputtered on to the Si(100) substrate.

2-3-2 Analysis equipments

SEM (Scanning Electron Microscopy/ JEOL JSM-6500F)

SEM shows the morphology of material in the range of 20 to 500,000 times their normal size. The SEM supplies a quick, clear, three-dimensional view of a specimen, and it is very useful in analyzing morphology of material. A JEOL JSM-6500F scanning electron microscope operating at 15KV with a point-to-point resolution of 2nm was used for conventional SEM examinations.

HRTEM(High Resolution Transmission Electron Microscopy/ JEOL JSM-3010)

TEM shows a real space image on the atomic distribution in the nanocrystal, producing images in the range of 50 to 1,200,000 times.

A JEOL JSM-3010 transmission electron microscopy operating 300KV with a point-to-point resolution of 0.14nm was used for lattice imaging.

PL/Raman spectrum (Photoluminescence spectrum system, wavelength of laser is 266nm/ Raman spectrum system, wavelength of laser is 632.8nm)

Photoluminescence and Raman spectroscopy has long been recognized as an analytical tool. They were used for analyzing structural characteristic.

XRD (X-ray powder diffraction, Cu $K_{\alpha 1}$ radiation, $\lambda = 1.542 \text{ \AA}$)

X-ray powder diffraction produces the analyzing of structure of material. It is powerful in recognizing the material and structure.

Chapter 3: Synthesis of one-dimension GaN nanostructure encapsulate inside carbon nanotube

3-1 Experiment Method

Quasi 1-D GaN-CNT nanocables were synthesized by using a thermal chemical vapor system. TMG was used as a Ga precursor. C₂H₂ and NH₃ were used as C and N precursors. Silicon (100) (P type) wafers containing the native oxide layer coated 5nm-Au were used as the substrate. Au-catalyzed metal-organic chemical vapor deposition synthetic reaction was executed. The substrate was transferred into the hot zone inside the quartz tube evacuated to a base pressure 5×10^{-5} .

Quartz tube was divided into three zone which were kept at 850 °C, 800 °C, 750 °C and the tube was held in the flowing ammonia (200 standard cubic centimeters per minute), TMG was kept at the low temperature in -12 °C bath and C₂H₂ (50 and 25 standard cubic centimeters per minute) at the reaction temperature for 2 hr and the base pressure is 100 torr. With C₂H₂ flow rate increasing, the diameter of nanowires becomes larger. The temperature of the reactor was set at 800 °C increased at a rate of 16 °C/min from room temperature to the reaction temperature. The experimental setup for GaN@CNT nanowires is described schematically in Fig. 3-1.

SEM was used to examine the morphology of 1-D nanostructure. The structure and components of the nanostructure is characterized by X-ray diffraction pattern, Raman spectrum and photoluminescence spectrum. The fine nanostructure dispersed on the carbon film coating by a Cu grid

and analyzed by high resolution transmission electron microscopy.

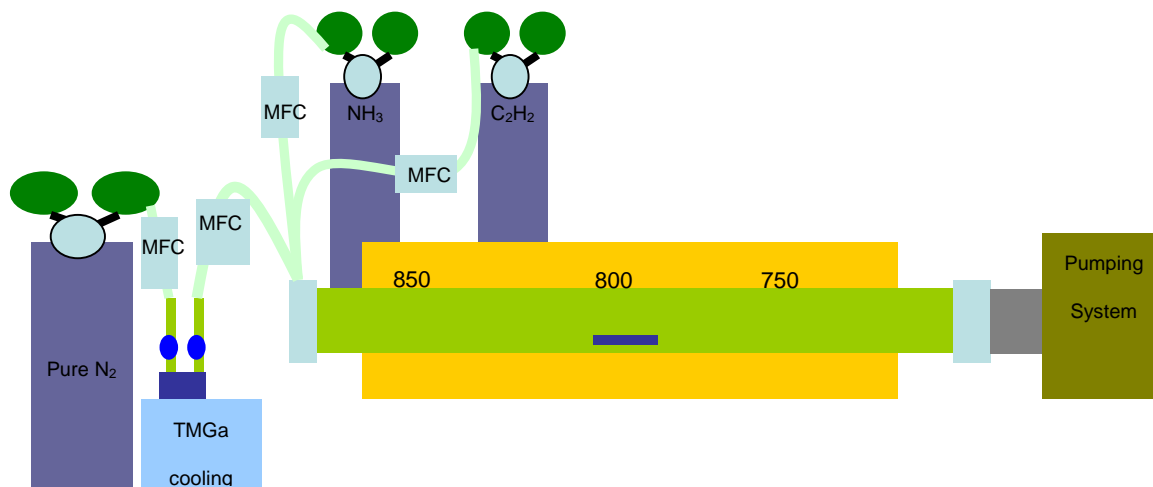


Fig.3-1 Schematic diagram of the setup for preparing the GaN@CNT and needly GaN nanowires

3-2 Results and Discussion

SEM image shows an overview of the nanostructure-filled CNT coverage on a gold coated (100) plane silicon substrate with C₂H₂ (25sccm) reveals that the product is high-density nanowires (Fig. 3-2(a)). The length of nanowires taken from SEM image is about 3-6 μ m (Fig. 3-2(b)). The nanowires are look like grassland. We can observe the wire-like nanostructure in the CNT obviously from magnified SEM images (Fig. 3-2(c)) and the diameter of nanostructure-filled CNT taken from SEM image is about 20-50nm. The nanowires diameter is confined by the shell of CNT and the diameter similar to the inside diameter of CNT.

In the X-ray diffraction pattern (Fig. 3-3), the reflections can be indexed to hexagonal wurtzite cell. The cell parameters of $a=3.180 \text{ \AA}$ and

$c = 5.184 \text{ \AA}$, revealing the deposited product is hexagonal GaN. A sharp peak position at $2\theta = 25.6^\circ$ is assigned to the CNT.

The high-resolution TEM (HRTEM) images reveal the detailed features for an individual GaN@CNT nanowire. Fig. 3-4(a) shows that the nanostructure is coated several sheets of the graphitic layers. It was found that the nanowires exhibit cable-like structure with uniform inner diameter ranging from 15 to 20 nm which is taken from HRTEM image and that is similar to the nanorod within CNT

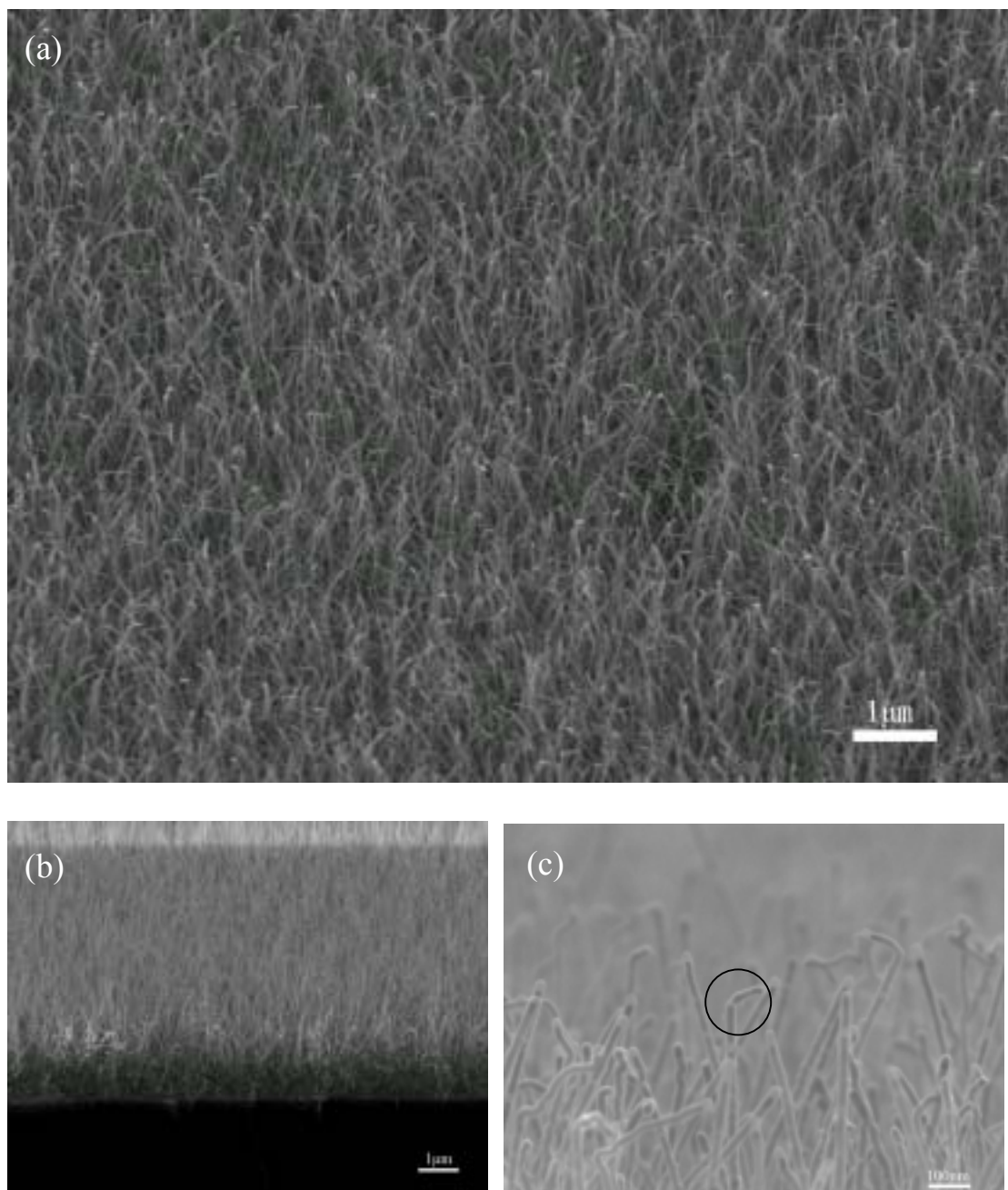
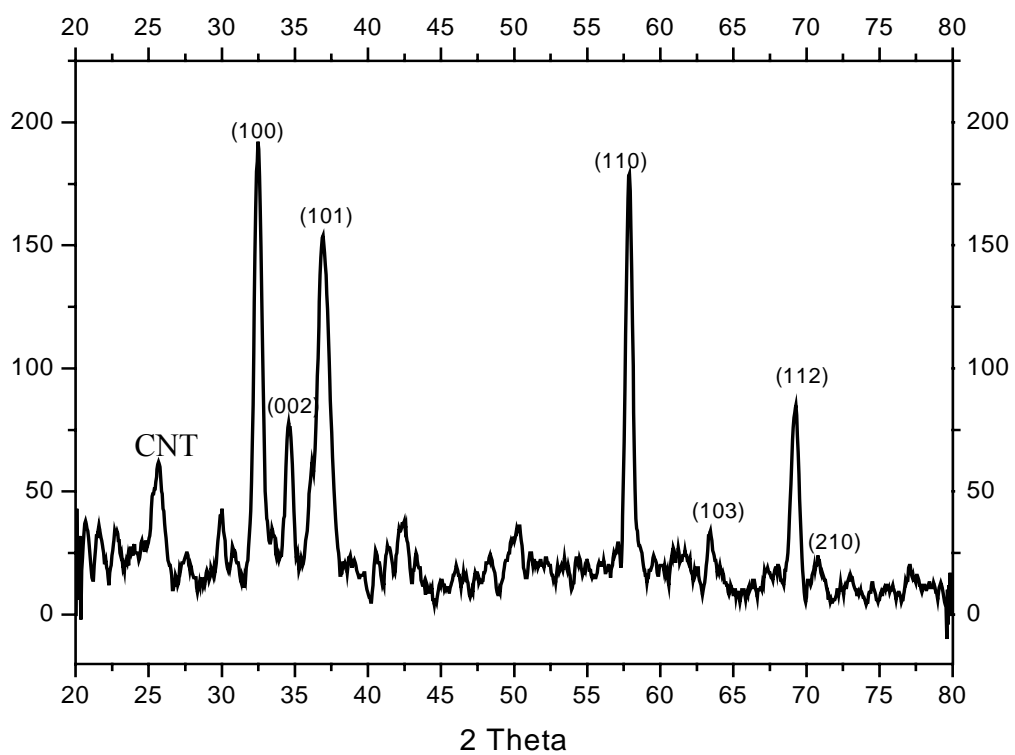


Fig.3-2 SEM images of GaN@CNT with the relatively much amount of C_2H_2 (a) a tilt of plane view (b) cross-section (c) high-magnification images.



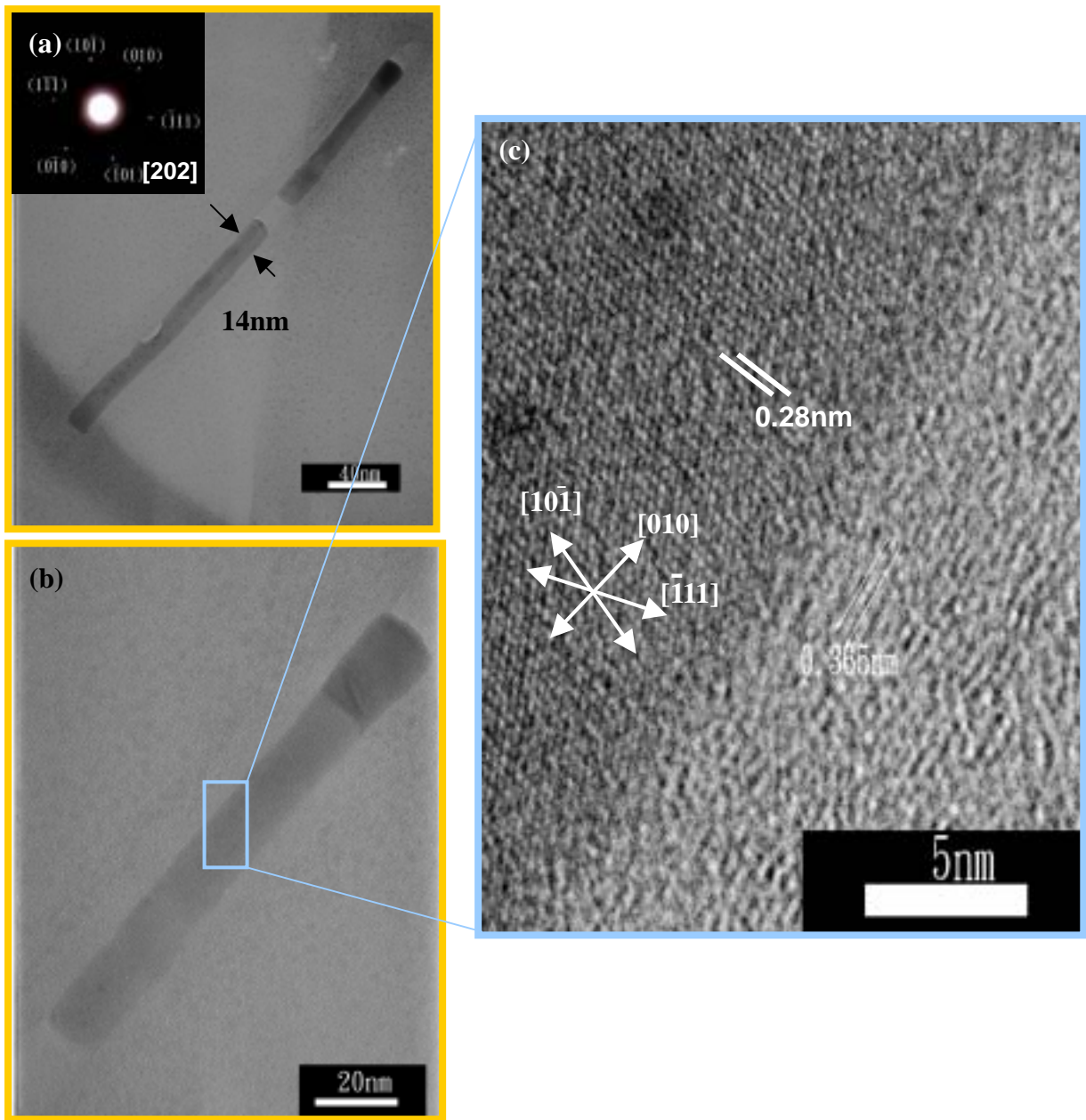


Fig.3-4 (a) GaN nanorod is coated several sheets of the graphitic lays; the inset is the corresponding diffraction patterns (b) high-magnification of a section of GaN nanorod, (c) The interface of GaN and CNT.

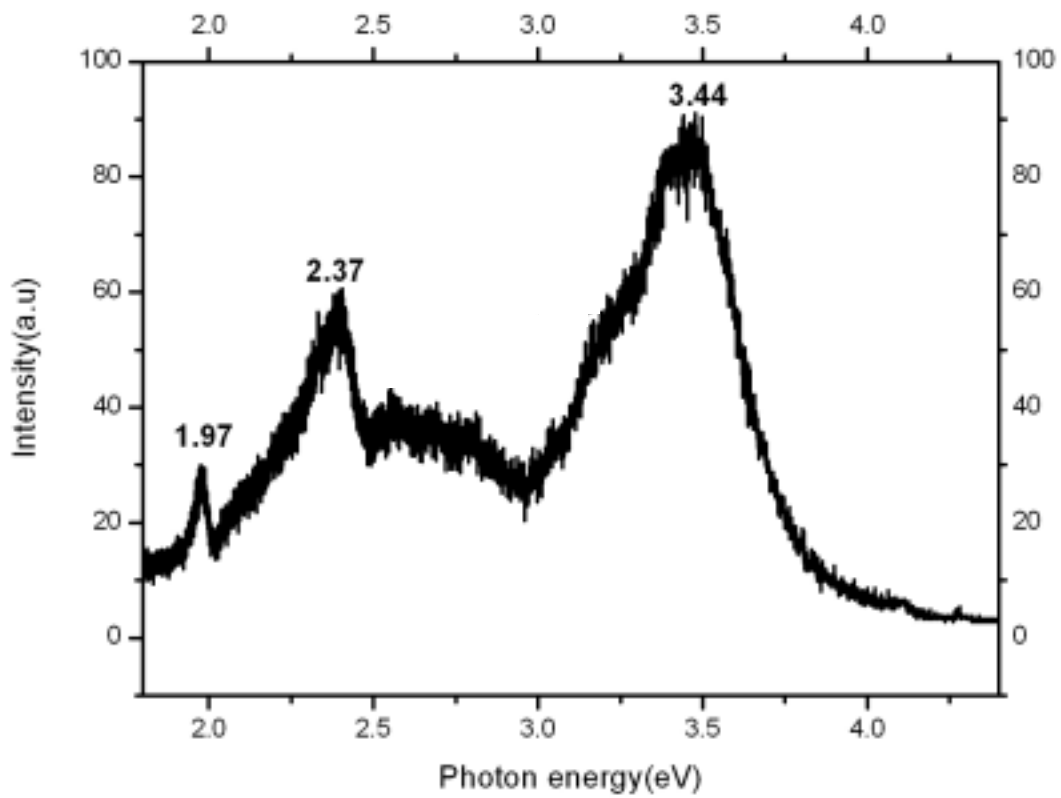


Fig.3- 5 Typical PL spectra from GaN@CNT nanowires

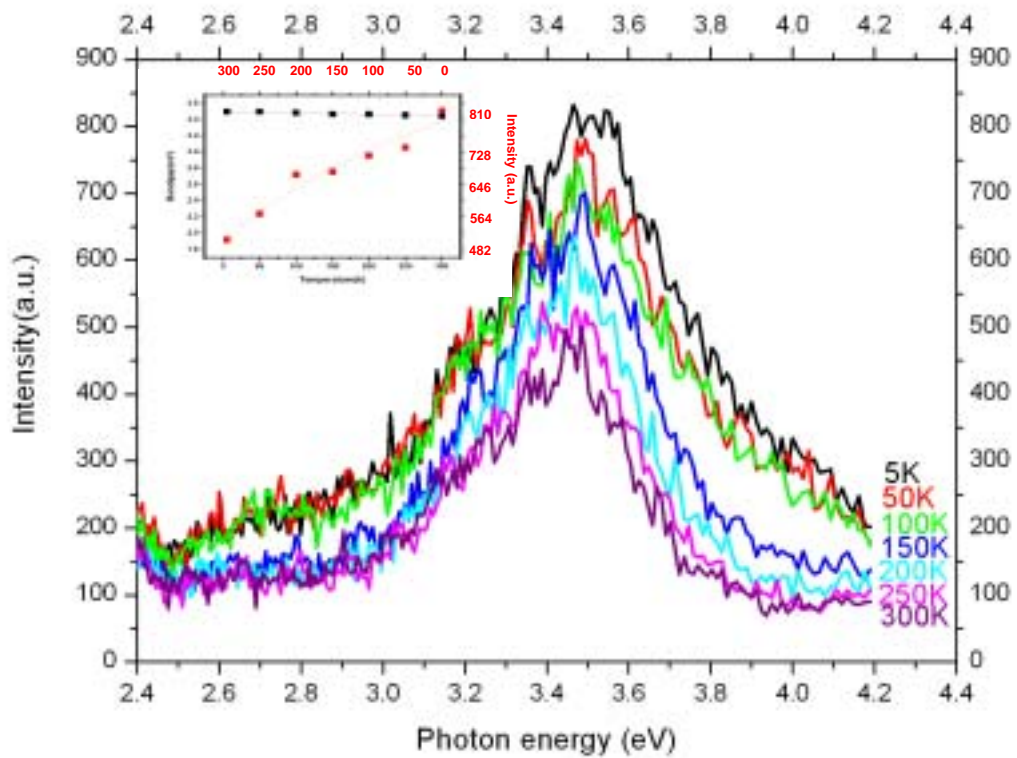


Fig.3-6 Temperature dependence of photoluminescence spectrum

which is confined by CNT. The inset of Fig 3-4(a) is the corresponding diffraction patterns, which also can be indexed to hexagonal wurtzite GaN. The incidence direction of the electron beam is along $\langle 202 \rangle$ direction. The axis direction of the GaN nanorod is $[010]$. High-magnification shows a section of GaN nanorod (Fig. 3-4(b) (c)), which is a lattice resolved HRTEM image of a GaN nanorod. The distance between two lattice planes and the distance between two graphite layers are as shown in a high-magnification image of GaN@CNT. The clear cross lattice fringes observed in the core indicated that GaN nanorods have a single crystal structure. The shell of the CNT consists of about 18 graphite concentric layers with a uniform spacing of 0.365nm between two consecutive layers.

Fig.3-5 shows a PL spectrum obtained for the GaN@CNT nanowire at room temperature. The PL spectrum consists of one strong peak at 3.44 and another emission peaks at 2.37 and 1.97eV. The peak position at 3.44eV comes from the band to band emission. The blue shift of the band-gap emission compare with the band-gap of bulk GaN 3.36eV. Fig.3-6 shows the PL spectra at seven different temperatures from 5 to 300K. The PL peak positions are 3.49eV at 5K and 3.44eV at 300K.

Fig.3-7(a) shows the GaN@CNT nanowires with 25sccm C_2H_2 . The wire is longer and thinner than relatively a larger amount of C_2H_2 source. It was found that the nanowire has length up to several micrometers and diameter ranging from 15 to 20nm (Fig. 3-7(b)(c)). Nanowires with diameters less than 10nm were also observed. We also can observe that a few GaN nanostructure in the CNT from Fig. 3-7(c).

In the X-ray diffraction pattern (Fig.3-8), the reflections can be indexed to hexagonal wurtzite cell. The cell parameters of $a=3.183 \text{ \AA}$ and $c=$

5.173 Å, revealing the deposited product is hexagonal GaN. We can not observe the peak at the position, $2\theta=25.6^\circ$, of CNT. We make a guess at that the sum of graphite layer is fewer than thick GaN@CNT nanowires.

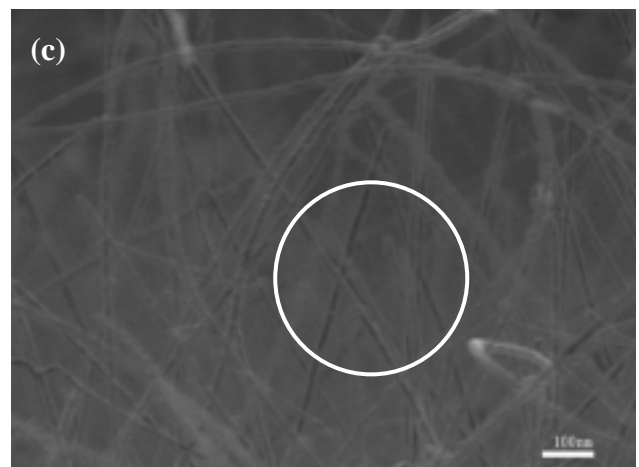
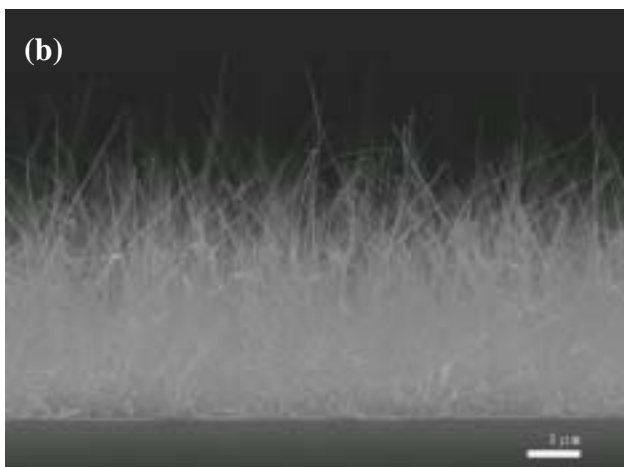
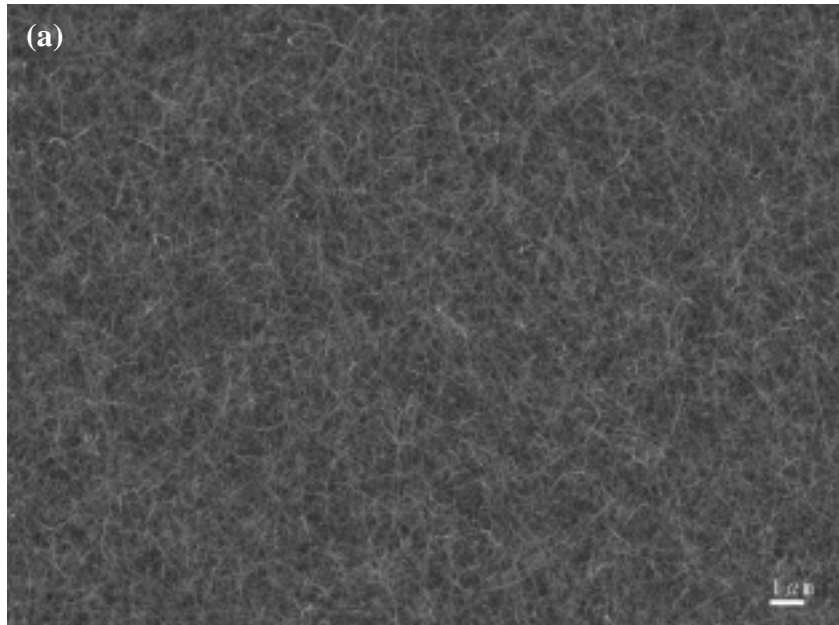


Fig.3-7 Typical SEM image (a) high-density nanowires (b) coress-section of GaN@CNT nanowire (c) high-magnification image and the range of circle shown the nanostructure within the CNT

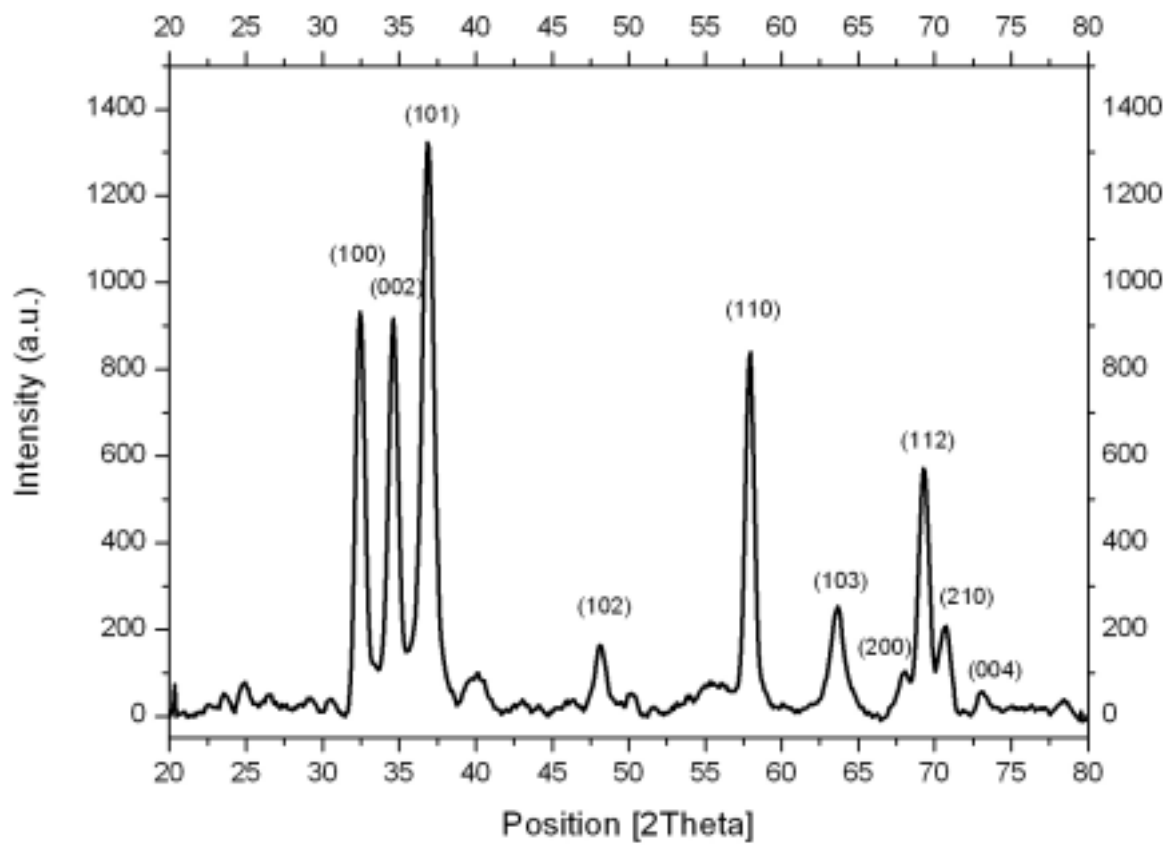


Fig.3-8 The X-ray diffraction pattern of the nanowire

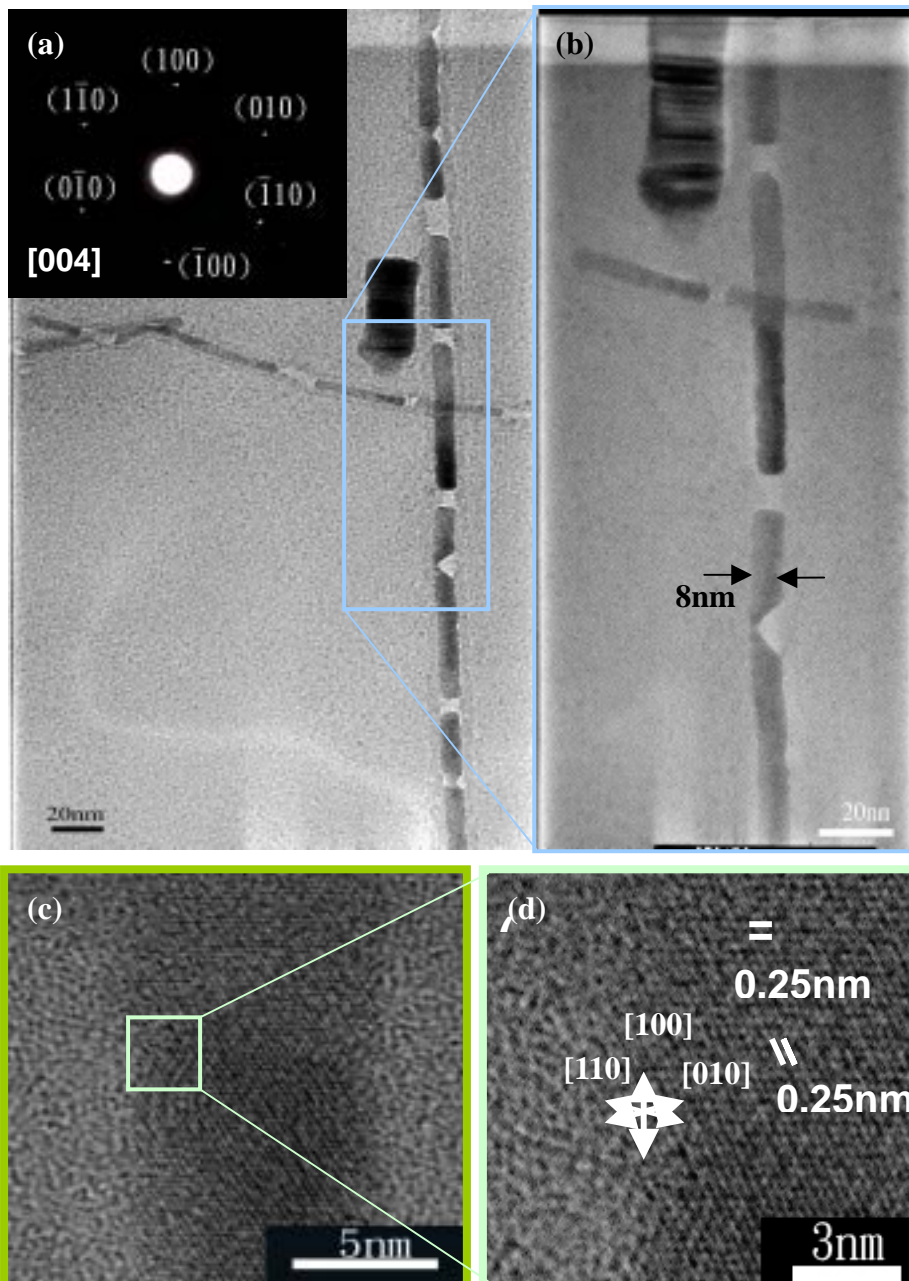


Fig.3-9 HRTEM image of GaN@CNT (a) low-magnification image; the diffraction pattern of nanowire in inset (b)(c) the diameter of GaN core is about 8nm (d) the atomic resolved lattice

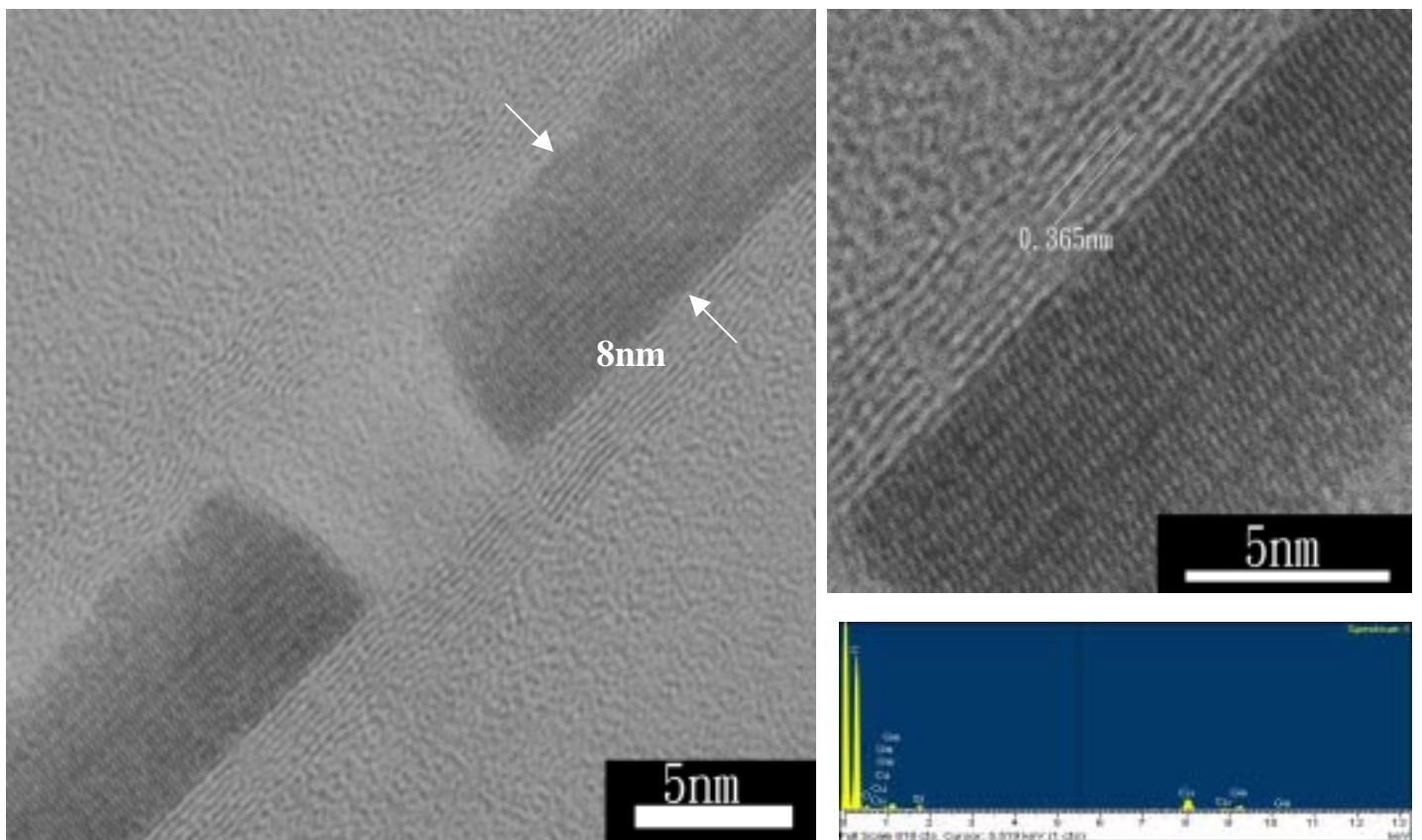


Fig.3-10 An individual GaN@CNT nanowire HRTEM image

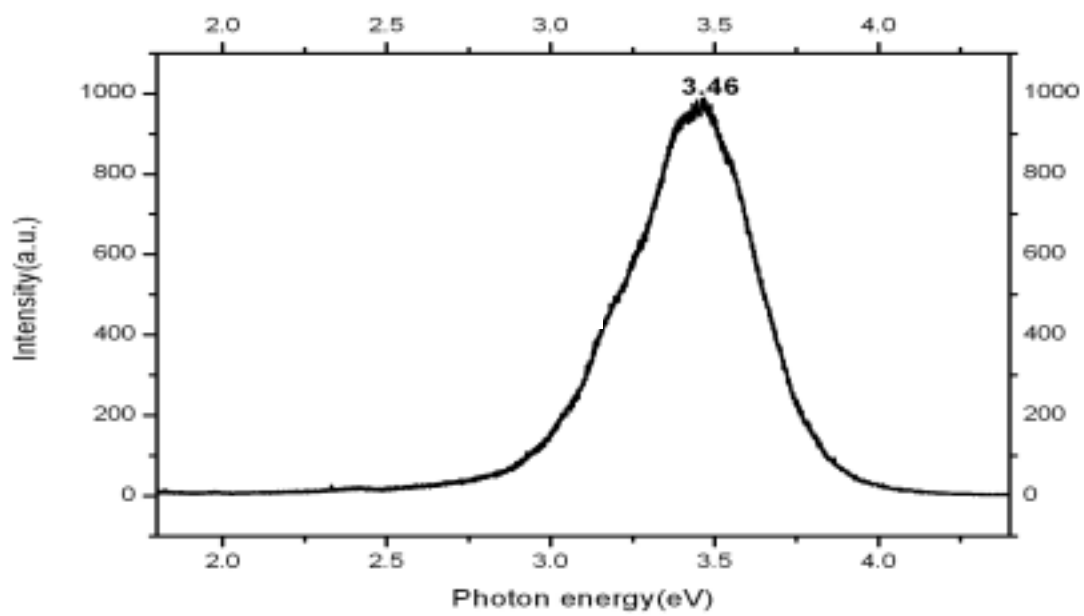


Fig.3-11 Typical PL spectra from GaN@CNT nanowires

Fig. 3-9(a) displays a low-magnification TEM image of nanowire. It is quite obvious that GaN core packed in CNT and the inset indicating exactly the (100) lattice plane perpendicular to the wire axis and with the $\langle 004 \rangle$ axis parallel to the electron beam. Fig. 3-9(b)(c) show a TEM image of GaN@CNT nanowire, where the detail structure of GaN core can be clearly seen. The GaN nanorods have diameters, 8nm, less than the Bohr exciton radius for GaN, 11nm. Fig.3-9(d) shows the atomic resolved lattice. The HRTEM image of crystalline GaN core is shown in Fig.3-9(c). In the image, the lattice space of about 0.25 nm corresponds to the distance between two (100) planes.^[45] Fig.3-10 shows clearly that the shell of the CNT consists of about 8 graphite concentric layers with a uniform spacing of 0.365nm between two consecutive layers and a GaN nanostructure-filled CNT. We also can find the nanowires consists mostly of Ga from EDS spectra. Typical PL spectra come from GaN@CNT nanowires as shown in Fig. 3-11. The peak position is at 3.47eV at room temperature. The peak comes from the band to band emission. The blue shift of the band-gap emission compare with the 3.36eV and 3.43eV band of bulk GaN and thick GaN@CNT might be due to the quantum confined effect since a compresses stress of the lattice constant and the diameter of GaN nanorod is less than the Bohr exaction radius for GaN, 11nm. We can observe obviously that this sample has no yellow luminescence of defect at room temperature. Fig.3-12 shows the PL spectra at seven different temperatures from 5 to 300K. The PL peak positions are 3.44eV at 5K and 3.39eV at 300K. Fig.3-13 shows the PL spectra taken from GaN@CNT nanowires with core sizes of 14nm (Fig.3-4) and 8nm (Fig.3-9), and GaN nanowires with a diameter of 36nm. We can observe obviously the quantum confinement effect from the blue-shift of the PL spectra.

The room temperature Raman scattering spectra of the GaN@CNT

nanowires are displayed in Fig.3-14 which shows the compare of two different conditions sample. In the spectrum of thick GaN@CNT, the peaks at 1339 and 1585 cm^{-1} and the peak of thin GaN@CNT is at 1335 and 1585 cm^{-1} which come from the CNT information. We also can observe the Si substrate information at 299, 517 and 953 cm^{-1} . We can not observe the peak of GaN. That might be due to GaN is direct band gap, and the phonon is not easy observed.

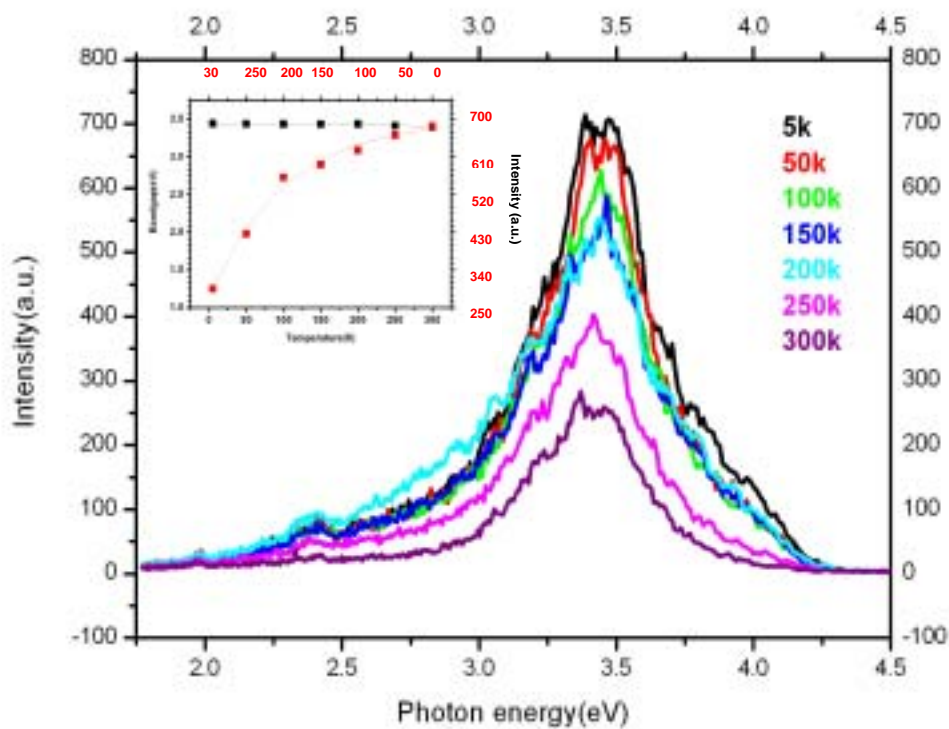


Fig.3-12 Temperature dependence of photoluminescence spectrum

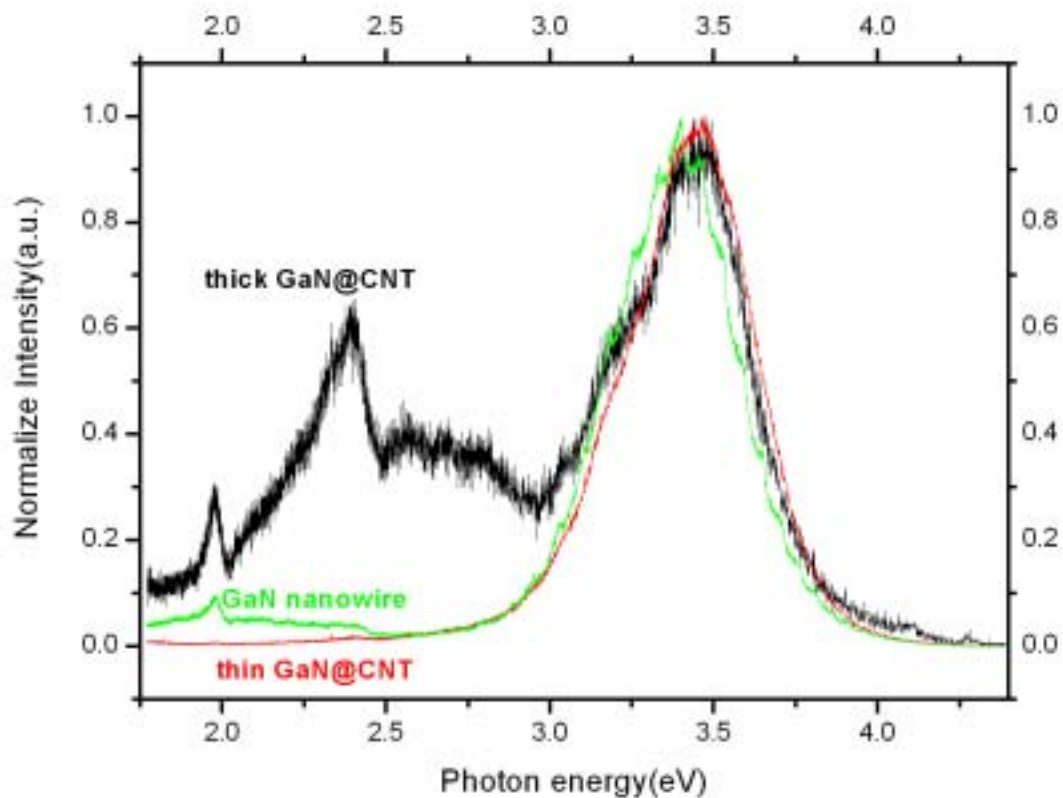


Fig.3-13 Blue-shift of photon energy

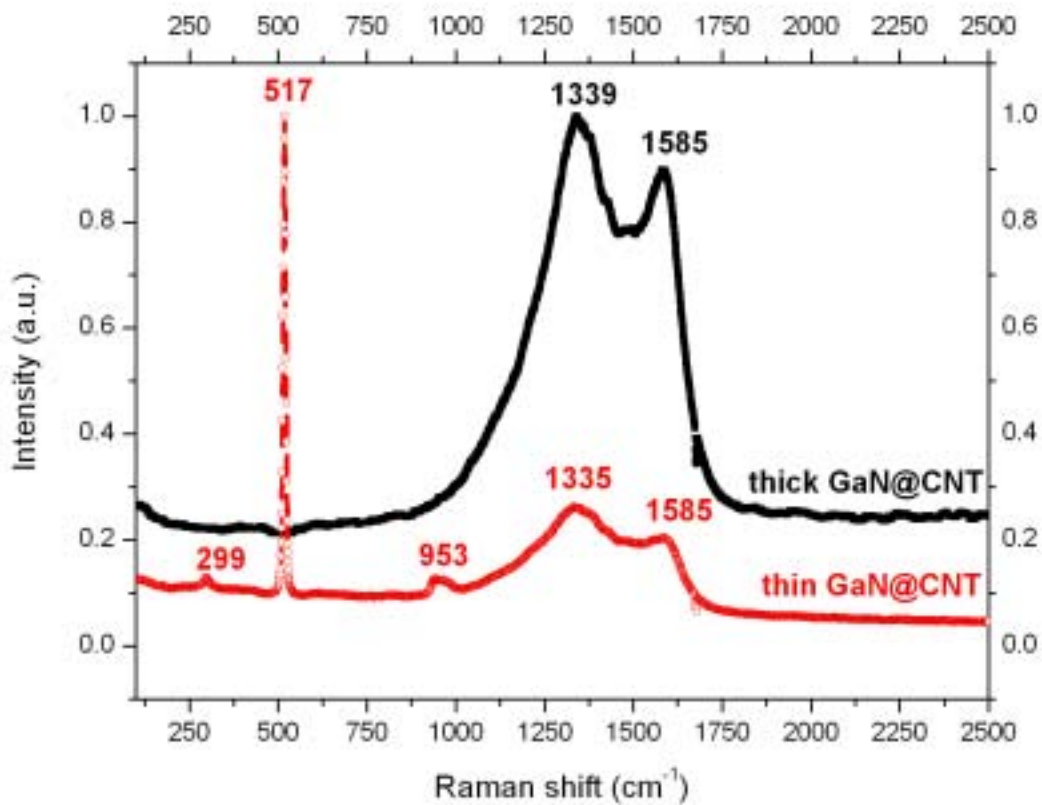


Fig.3-14 Raman spectrum of the GaN@CNT nanowires with different core sizes.

Chapter 4: Synthesis of GaN nanowire

4-1 Experiment Procedures

The experimental setup for GaN nanowire is described schematically as shown in Fig. 3-1. TMG and ammonia (150 standard cubic centimeters per minute) source were used as GaN nanowire precursors. Subsequent the reaction of GaN nanowires occurred at a substrate temperature of 750 and the base pressure is 100 torr keep the condition for 5 hr. TMG was kept at a cool bath in -12 . The second step of reaction was occurred under cooling down condition and close down gases.

SEM was used to examine the morphology of 1-D nanostructure. The structure and components of the nanostructure is characterized by X-ray diffraction pattern, Raman spectrum and photoluminescence spectrum. The fine nanostructure dispersed on the carbon film coating by a Cu grid and analyzed by high resolution transmission electron microscopy.

4-2 Results and Discussion

The SEM image shows in Fig. 4-1(a) gives an overview of the morphology of the synthesized product coverage on a gold coated (100) plane silicon substrate. The wire were observed from SEM image that have triangular cross-section with 30-50 nm widths and length about 2-5 μm . Fig.4-1(b)(c) shows the high-magnification images of plane view. We can observe the triangular cross section nanowire obviously in Fig.4-1(c). Fig.4-2(a) shows low-magnification image of cross section with 2-step nanowires and Fig.4-2(b)(c) show the high-magnification of GaN

nanowires. The second part of GaN is much smaller than most what we observe and we also can see which have some protrusions near the needle head. We also can find out the structure and elements of the 1-D nanostructure by X-ray diffraction pattern indexed in Fig.4-3. The structure of nanowires is hexagonal wurtzite and consists of GaN which can be analyzed by the peak positions. Strong peak at the (100), (002), (101), (102), (110), (103), (200), (112), (210) and (004) planes are seen for nanostructure GaN. The lattice constant of 2-step GaN nanowire is $a=3.180 \text{ \AA}$ and $c=5.177 \text{ \AA}$.

These nanowires were dispersed on Cu grid coated a graphite film to carry out additional structural and compositional analysis. Detailed structure information of individual 2-step GaN nanowire was obtained by using TEM image as shown in Fig.4-4. The TEM image showed that the products are relatively straight nanowire with diameter ranging from 31nm to 37nm, which are thicker than the needle head with 5 nm of diameter. The inset of Fig.4-4 shows as a selected-area electron diffraction pattern of the nanowire that can be indexed to the reflection of hexagonal GaN crystals. It is obviously indicating exactly the (-122) lattice plane perpendicular to the wire axis and with the $\langle 2-12 \rangle$ axis parallel to the electron beam. Fig.4-5(a) shows a TEM image of an individual GaN nanorod, which is a part of GaN nanowire, where the detail structure of GaN can be clearly seen. The body of nanowire has 36nm diameter and the needle head has 5nm diameter. Fig. 4-5(b)(c) shows a high-magnification TEM image of the nanorod, the distance between two continue lattice plane are 0.269 and 0.258nm separately. The EDS spectrum analysis reveals that the composite of nanowires is most of Ga as shown in Fig.4-6. The nanowires also can be inferred

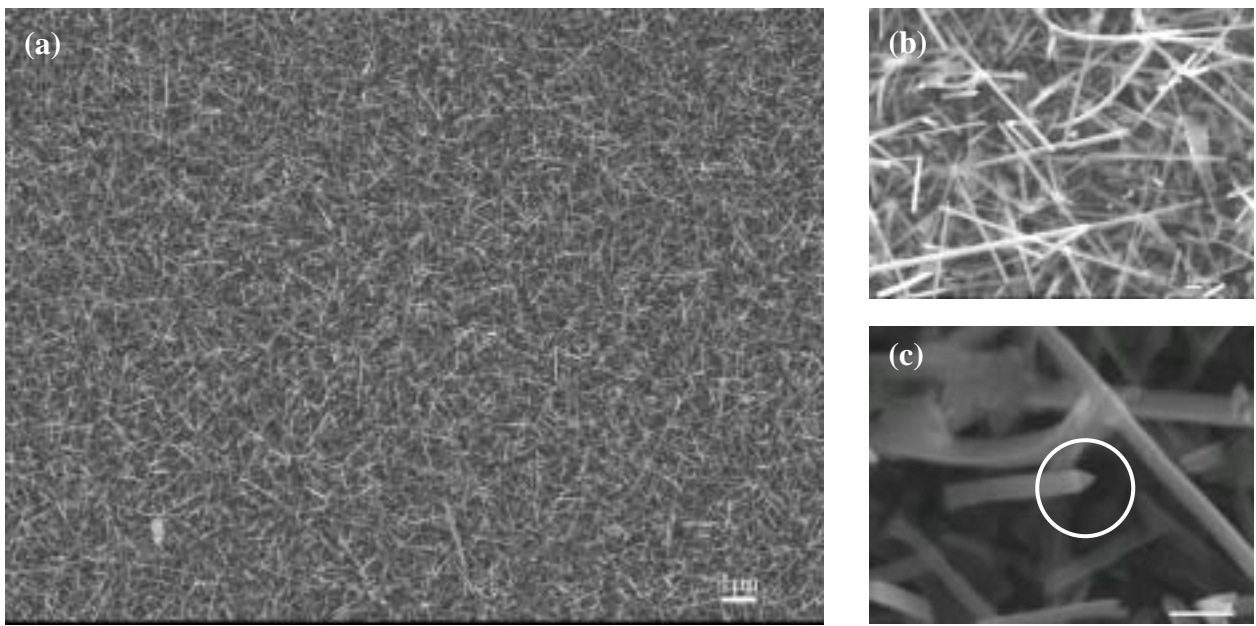


Fig.4-1 SEM images of GaN nanowire (a) morphology view (b) (c) high-magnification images of triangular GaN nanowires.

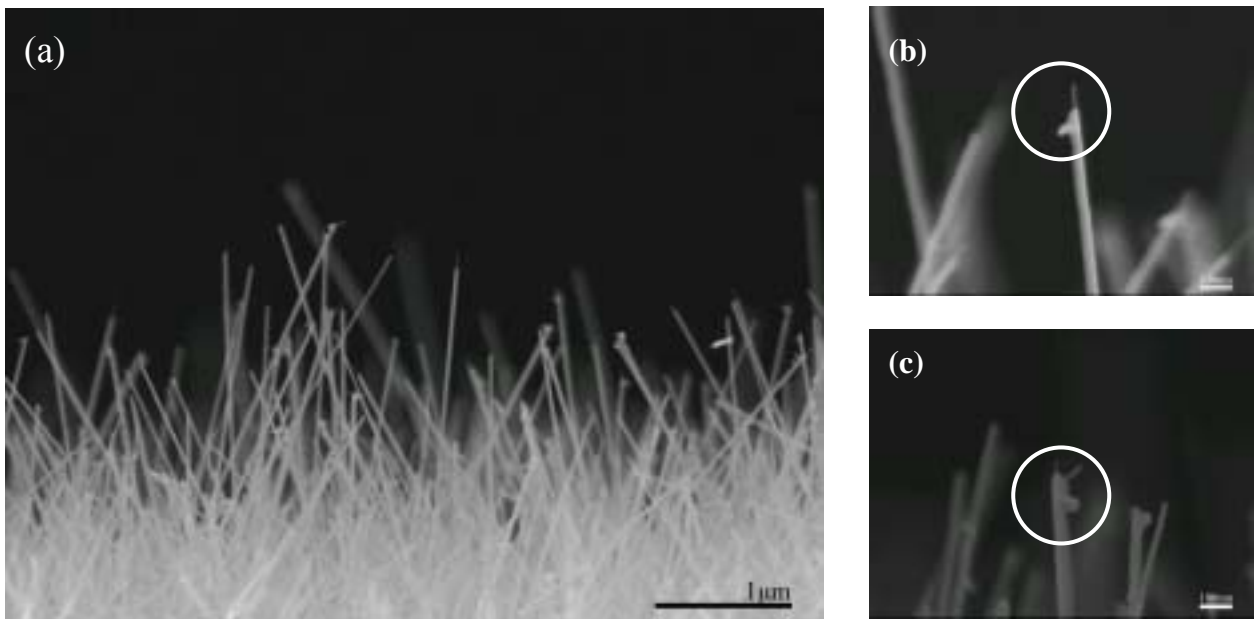


Fig.4-2 SEM images of GaN nanowires cross section (a) a large amount of GaN nanowire (b)(c) a needle-like structure upon the nanowire

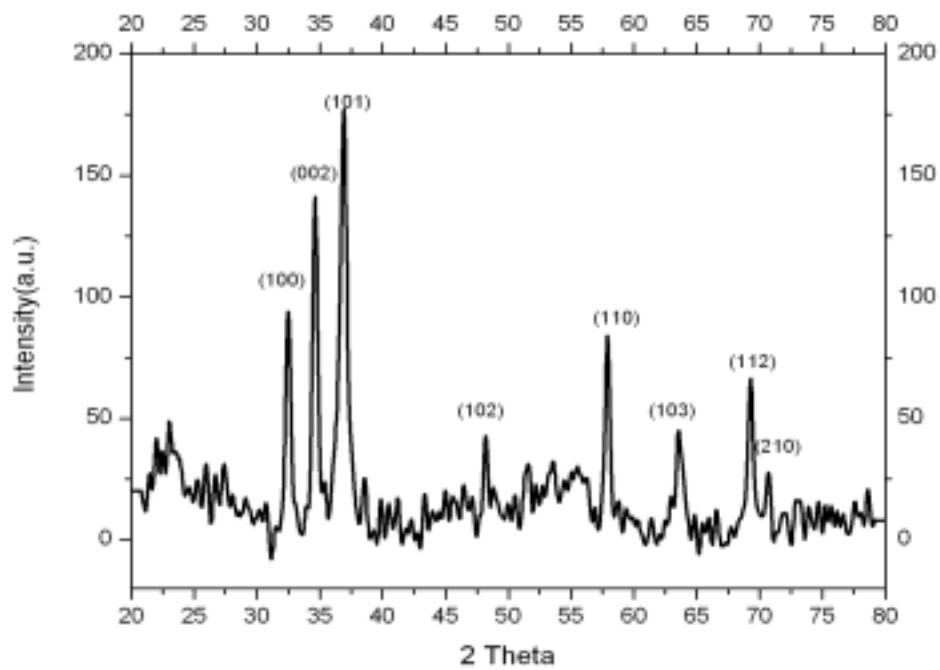


Fig.4-3 A range from 20° to 80° XRD pattern taken from the GaN nanowire.

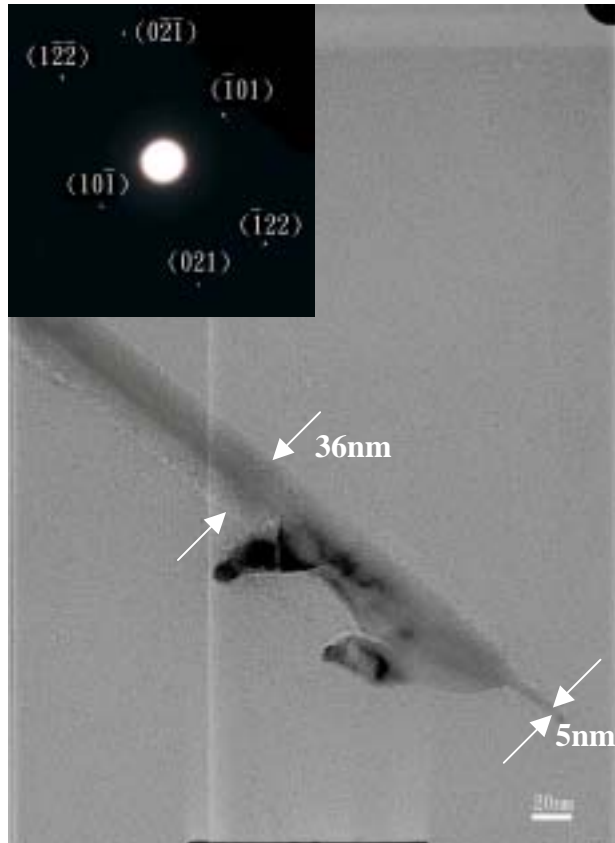


Fig.4-4 TEM image of full view; the inset is the diffraction pattern of the nanowire.

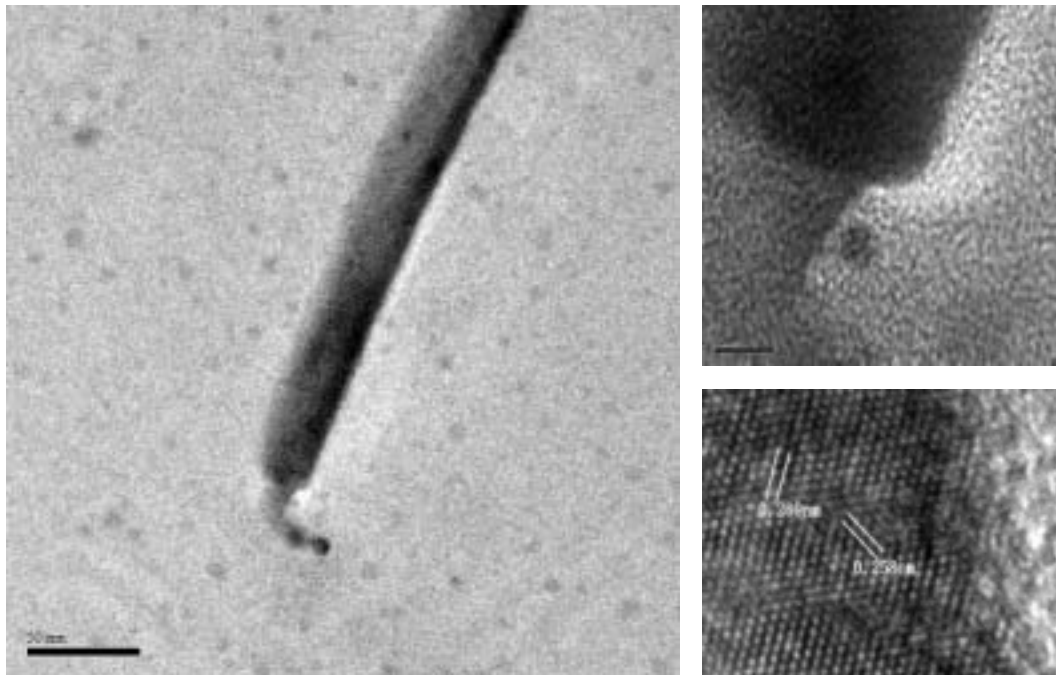


Fig.4-5 (a) An individual GaN nanowire image (b)(c) high-magnification image of GaN nanowire

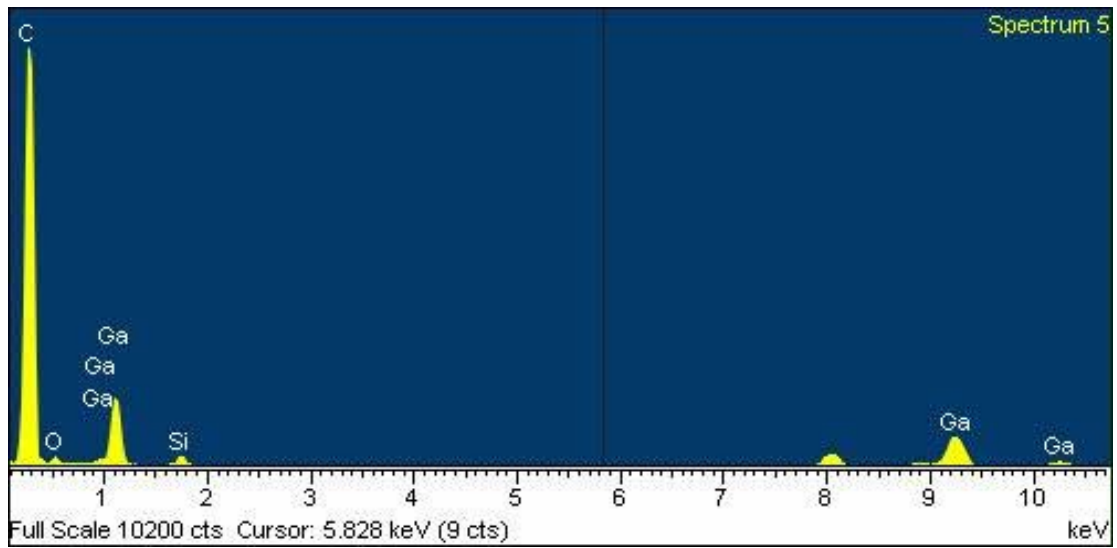


Fig.4-6 EDS of single GaN nanowire

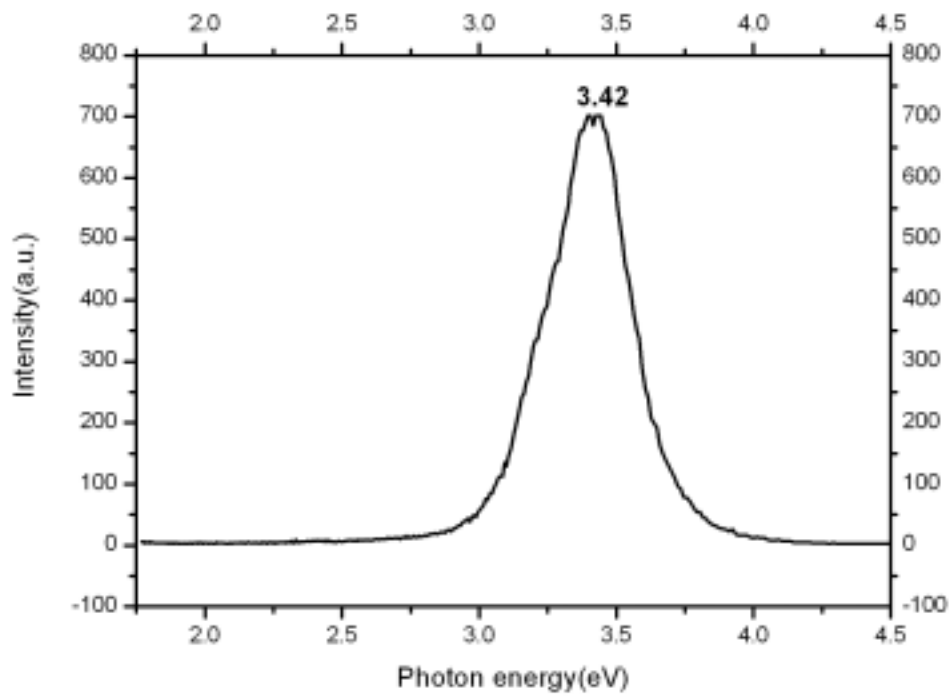


Fig.4-7 PL spectrum of GaN nanowire at room temperature

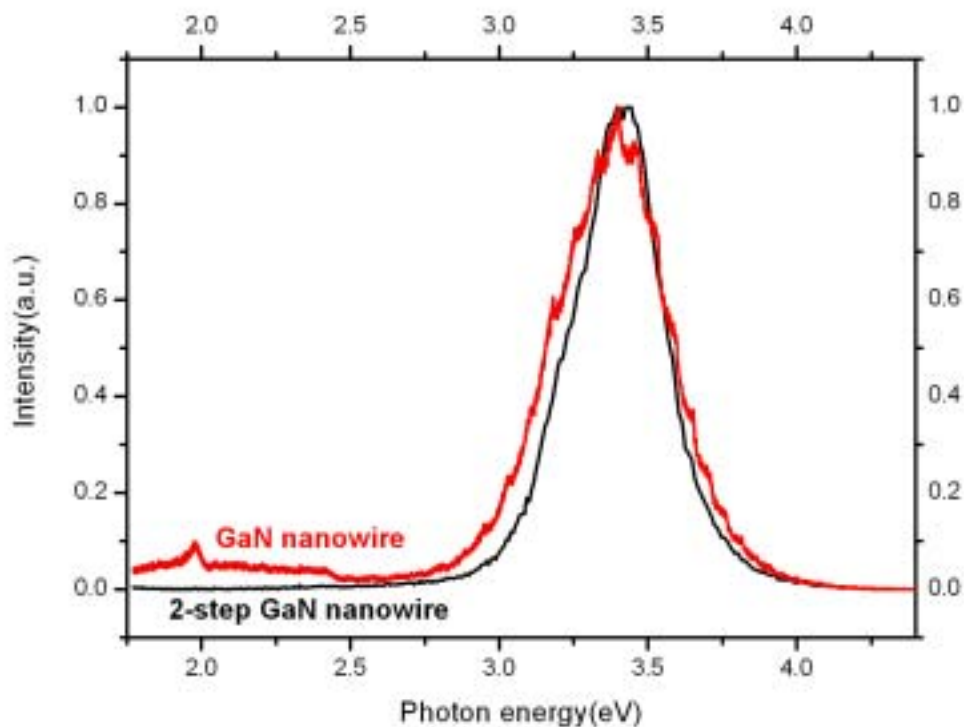


Fig.4-8 PL spectrum of GaN nanowires with diameter of 36 nm and 2-step GaN nanowires

from EDS data to include the majority composite of the nanowire is Ga.

Fig. 4-7 shows a PL spectrum obtained for the GaN@CNT nanowire at room temperature. The PL spectrum consists of one strong peak at 3.44eV as shown in Fig. 4-7. The peak position at 3.44eV comes from the band to band emission. The blue shift of the band-gap emission compare with the band-gap of bulk GaN 3.36eV. We can observe obviously that this sample has no yellow luminescences of defect at room temperature. Fig.4-8 shows the relationship of PL spectra between GaN nanowires and

2-step GaN nanowires. We can not observe obviously the quantum confinement effect from the analysis of spectra due to the second part GaN nanowires are too short. The room temperature Raman scattering spectra of the GaN@CNT nanowires are displayed in Fig.4-9. In the spectrum of 2-step GaN, most of the peaks indicate the Si substrate, including 297, 529 and 939 cm^{-1} . The peak of GaN at 225 cm^{-1} is the weak information of 2-step GaN nanowire.

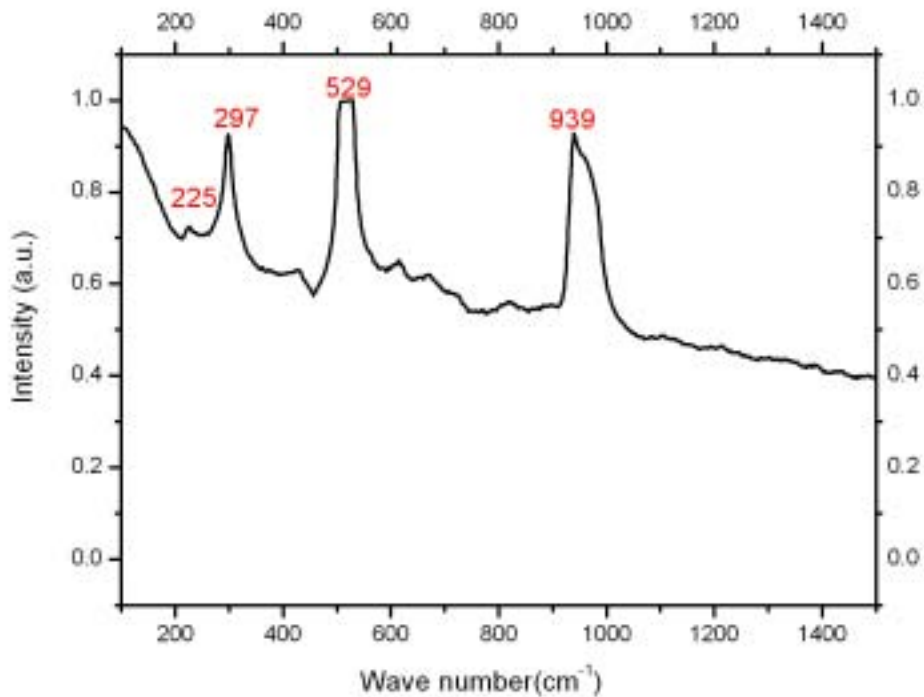


Fig.4-9 Raman scattering spectrum of needly GaN nanowires

Chapter 5: Conclusion

Carbon nanotubes (CNT) were used to confine the radial growth simultaneously growth of GaN and carbon nanotube. The presence of the wurtzite structure GaN nanowires encapsulated inside the cavity along the length of a multi-wall carbon nanotube by experiment result. In the experiment, the inner and outer diameters and GaN nanowire encapsulated inside the carbon nanotube were changed with the flow rate of C_2H_2 was controlled. The outer diameter of CNT is about 20-50 nm and the diameter of GaN nanowire is about 10-15nm while the flow rate of C_2H_2 was controlled to be 50sccm. The outer diameter of CNT is about 15-20 nm and the diameter of GaN nanowire is about 6-8nm while the flow rate of C_2H_2 was controlled to be 25sccm. The diameter of GaN nanowire is decreasing with the flow rate of C_2H_2 reduced and constrained by the inner diameter of CNT as well as the band-gap has blue-shift. The blue shift of the band gap emission (3.47eV) of thin GaN@CNT compared with the 3.44 or 3.36eV band of thick GaN@CNT or bulk GaN is attributed to quantum confined effect. Gold can not catalyze the growth of CNT is already knew ago, but we find that the carbon nanotube can be catalyzed by Ga in documents. Hence we suppose the growth of CNT was catalyzed by Ga-Au alloy and the sections of GaN nanowire were caused by the different speed of growth.

On the side, we synthesize GaN nanowire by 2-step method. The first part of GaN nanowire was synthesized at 750 and the second part was synthesized while the temperature cooling down. The GaN nanowire was

defined to be wurtzite structure from experiment result. The first part of the wire was observed from TEM image that has triangular cross section with 36 nm diameters and the second part of the wire was observed from TEM image that has 5nm diameter. The other quantum size GaN nanowires possess the 3.44eV band gap. We can not obviously find the quantum confined effect. Maybe is the quantum size structure smaller than the bulk. Hence we suppose that the synthesis of second part of GaN nanowire was catalyzed by using the minority of Au was not covered by nitrides as catalyst during cooling down.

In this study, the method of synthesizing GaN@CNT is efficiently to control the diameter of GaN nanostructure. That is efficiently and simply to synthesize a large amount of semiconductor materials possess quantum confinement effect.

Reference

- [1] Ko-Wei Change and Jih-Jen Wu, *J. Phys. Chem. B* **2002**, 106, 7796-7799.
- [2] Shuji Nakamura, Masayuki Senoh, and Takashi Mukai, *Appl. Phys. Lett.* 62 (19), 2390
- [3] Johnson, J. C.; Choi, H.; Knutsen, K. P.; Schaller, R. D.; Yang, P.; Saykally, R. J. *Nature Mater.* **2002**, 1, 106
- [4] Z. Zhong, F. Qian, D. Wang, and C. M. Lieber, *Nano Lett.* 3, 343, 2003
- [5] Han W.; Fan S.; Li Q.; Hu Y.; *Science* **1997**, 277, 1287
- [6] Han W.; Redlich P.; Ernst F.; Ruhle M. *Appl. Phys. Lett.* **2000**, 76, 652
- [7] Duan X.; Lieber C. M. *J. Am. Chem. Soc.* **2000**, 122, 188
- [8] Li J. Y.; Chen X. L.; Qiao Z. Y.; Cao Y. G.; Lan Y. C. *J. Cryst. Growth* **2000**, 213, 408.
- [9] Han, W.-Q.; Zettl, A. *Appl. Phys. Lett.* **2002**, 80, 303
- [10] Chen X.; Li J.; Cao Y.; Lan Y.; Li H.; He M.; Wang C.; Zhang Z.; Qiao Z. *Adv. Mater.* **2000**, 12, 1432
- [11] Chen C.-C.; Yeh C.-H.; Chen C.-H.; Yu M.-Y.; Liu H.-L.; Wu J.-J.; Chen K.-H.; Chen L.-C.; Peng J.-Y.; Chen Y.-F. *J. Am. Chem. Soc.* **2001**, 123, 2791.
- [12] Zhang J.; Zhang L. D.; Wang X. F.; Liang C. H.; Peng X. S.; Wang Y. *W. J. Chem. Phys.* **2001**, 115, 5714.
- [13] Lee M. W.; Twu H. Z.; Chen C.-C.; Chen C.-H. *Appl. Phys. Lett.* **2001**, 79, 3693

- [14] Seo H. W.; Bae S. Y.; Park J.; Yang H.; Park K. S.; Kim S. *J.Chem. Phys.* **2002**, 116, 9492
- [15] Kim H.-M.; Kim D. S.; Park Y. S.; Kim D. Y.; Kang T. W.; Chung K. S. *Adv. Mater.* **2002**, 14, 991
- [16] J. Black, H. Lockwood, and S. Mayburg, "Recombination Radiation in GaAs," *J. Appl. Phys.*, **1962**, **34** , p. 178
- [17] M.G. Craford, "LEDs Challenge the Incandescents," *IEEE Circuits and Dev.*, 8 **1992**, p. 25.
- [18] Shuji Nakamura and Gerhard Fasol, "The Blue Laser Diode – GaN Based Light Emitters and Lasers" , Springer Verlag Berlin Heidelberg, **1997**
- [19] S. Strite and H. Morkoç, "GaN, AlN, and InN: A Review," *J. Vac. Sci. Technol.*, B10 **1992**, p. 1237.
- [20] Ko-Wei Chang and Jih-Jen Wu*, "Low-Temperature Catalytic Synthesis of Gallium Nitride Nanowires, " *J. Phys. Chem. B* **2002**, 106, 7796-7799
- [21] Goldberger, J.; He, R.; Zhang, Y.; Lee, S.; Yan, H.; Choi, H. J.; Yang, P. *Nature* **2003**, 422, 599.
- [22] Huang, Y.; Duan, X.; Cui, Y.; Lieber, C. M. *Nano Lett.* **2002**, 2, 101
- [23] Choi, H.; Johnson, J.; He, R.; Lee, S.; Kim, F.; Pauzuskie, P.; Goldberger, J.; Saykally, R.; Yang, P. *J. Phys. Chem. B* In press, **2003**.
- [24] Johnson, J. C.; Choi, H.; Knutsen, K. P.; Schaller, R. D.; Yang, P.; Saykally, R. *J. Nature Mater.* **2002**, 1, 106
- [25] S. Nakamura, T. Mukai, M. Senoh, *Jpn. J. Appl. Phys.* **1991**, 30, L1998; S. Nakamura, M. Senoh, N. Iwasa, S. Nagahama, *ibid.* **1995**, 34, L797.

- [26] R. Dingle, K. L. Shaklee, R. F. Leheny, R. B. Zetterstorm, *Appl. Phys. Lett.* **1971**, 19, 5
- [27] M. Asif Khan, D. T. Olson, J. M. Van Hove, and J. N. Kuznia, *Appl. Phys. Lett.*, **1991**, 58, 1515.
- [28] Nakamura, *S. Mater. Res. Soc. Proc.* **1996**, 449, 1135
- [29] Brus, *L. E. J. Phem. Chem.* **1994**, 98, 3575
- [30] Rupp, J.; Birringer, R.; *Phys. Rev.*, **1987**, B36, 7888.
- [31] Hellstern, E.; Fecht, H.; Fu, Z.; Johnson, W. L. *Appl. Phys. Lett.*, **1989**, 65,305.
- [32] Horvath, J. Diffus. Defect. Data: *Defect. Diffus. Forum*, **1989**, 66, 207
- [33] Horvath, J.; Birringer, R.; Gleiter, H. *Solid. State. Commun.* **1987**, 62, 319
- [34] Birringer, R.; Hahn, H.; Hofler, H. J.; Karch, J.; Gleiter, H. Diffus. Defect. Data: *Defect. Diffus. Forum*, **1988**, 59, 17
- [35] Gleiter, H. *Prog. Mater. Sci.*, **1989**, 32,223.
- [36] Wildoer, Jeroen; et. al, *Nature* **391** p59 1998
- [37] Z. W. Pan; S. S. Xie; B. H. Chang; C. Y. Wang; L. Lu; W. Liu; W. Y. Zhou; W. Z. Li; L. X. Qian, *Nature Volume* **394** Number 6694 Page 631 - 632 (1998)
- [38] Jeroen W. G. Wilder; Liesbeth C. Venema; Andrew G. Rinzler; Richard E. Smalley; Cees Dekker; *Nature* **391**, 1998, 6662, 59-62
- [39] A.C. Dillon, K.M. Jones, T.A. Bekkedahl, C.H. Kiang D.S. Bethune and M.J. Heben, *Nature*, **386**, 1997, 377.
- [40] Brigitte Vigolo, Alain Pénicaud, Claude Coulon, Cédric Sauder, René Pailler, Catherine Journet, Patrick Bernier, and Philippe Poulin

Science, **290**, 2000, 1331

[41] H. MorkoG, S. Strite,a) G. B. Gao, M. E. Lin, B. Sverdlov, and M.

Burns, *J. Appl. Phys.*, **76 (3)**, 1 August 1994, 1363 *J. Appl. Phys.*

[42] 梁其輝，表面鈍化可溶性氮化鎵奈米晶體的合成，碩士論文，

台灣，1998。

[43] http://elearning.stut.edu.tw/m_facture/Nanotech/Web/ch8.htm

[45] Byeongchul Ha, Sung Ho Seo, Jung Hee Cho, Chong S. Yoon, Jinkyoungh Yoo, Gyu-Chul Yi, Chong Yun Park,| and Cheol Jin Lee*, *J. Phys. Chem. B*, Vol. 109, 11096